JAERI-M
9992

PRELIMINARY ANALYSIS OF THE EFFECT OF THE GRID SPACERS ON THE REFLOOD HEAT TRANSFER

February 1982

Jun SUGIMOTO and Yoshio MURAO

日本原子力研究所
Japan Atomic Energy Research Institute

JAERI-Mレポートは，日本原子力研究所が不定期に公刊している研究報告書です。
入手の問合わせは，日本原子力研究所技術情報部情報資料課（〒319-11茨城県那珂郡東海村）あて，お申しこしください。なお，このほかに財団法人原子力弘済会資料センター（〒319-11 茨城県那珂郡東海村日本原子力研究所内）で複写による実費頒布をおこなっております。

JAERI-M reports are issued irregularly.
Inquiries about availability of the reports should be addressed to Information Section, Division of Technical Information, Japan Atomic Energy Research Institute, Tokai-mura, Naka-gun Ibaraki-ken 319-11, Japan.

編集兼発行　日本原子力研究所
印　　刷　(株)原子力資料サービス

JAERI-M 9992

Preliminary Analysis of the Effect of the Grid Spacers on the Reflood Heat Transfer

Jun SUGIMOTO and Yoshio MURAO

Division of Reactor Safety,
Tokai Research Establishment, JAERI

(Received January 28, 1982)

The results are described about the preliminary analysis of the effect of the grid spacers on the heat transfer during reflood phase of a PWR LOCA.

Experiments at JAERI and other facilities showed substantial heat transfer enhancement near the grid spacers. The heat transfer enhancement decreases with the distance from the grid spacers in the downstream region of the grid spacers. Several mechanisms are discussed about the heat transfer enhancement near the grid spacers. A model of a coalescence of the water droplets downstream the spacers is proposed based on the review of the experimental data. The heat transfer correlation for the saturated film boiling is utilized to quantify the heat transfer augmentation by the grid spacers.

Keywords: PWR LOCA, Reflood, Heat Transfer, Two-phase Flow, Grid Spacer.

JAERI－M 9992

再冠水期熱伝達に与えるグリッドスペーサの影響についての予備解析

日本原子力研究所東海研究所安全工学部
杉本　純・村尾良夫

（1982年1月28日受理）

本報は，PWR－LOCA時の再冠水過程における炉心内熱伝達に与えるグリッドスペーサの影響についての予備解析結果をまとめたものである。

原研における再冠水実験等においてグリッドスペーサの近傍における熱伝達率の増加が観測されている。熱伝達率はグリッドスペーサの下流側においてグリッドスペーサからの距離と共に減少している。グリッドスペーサ近傍における熱伝達率増加機構について考察し，実験データに基づいたグリッドスペーサ下流での液滴合体モデルを提案した。さらに飽和膜沸騰熱伝達相関式に基づいて，グリッドスペーサによる増加熱伝達率の定量的評価を行った。

Contents

目　　次

List of Tables and Figures

List of Tables and Figures in Appendix A

1. Introduction

1.1 Background

In a reflood phase of a PWR LOCA, it is important to evaluate the heat transfer from the fuel rods to the coolant in the core to evaluate the maximum temperature of the rods. Several experiments have been conducted to investigate the phenomena during the reflood phase. FLECHT[1] correlation derived from the FLECHT experiments[2] is utilized for the licensing calculation. Heat transfer correlation by Murao and Sugimoto[3] has been obtained based on the small reflood experiment at JAERI[4].

Figure 1.1 shows a typical responses of the temperature and the heat transfer coefficient of the rod obtained at JAERI's reflood experiment. The test section bundle of the experiment consisted of full length 4×4 electrically heated rods. The point A, which corresponds to a maximum temperature, is called a turnaround point, and the point B is called a quench point.

According to the results of the experiments, the local heat transfer downstream of the quench front is affected by the existence of the grid spacers to some extent[3]. Figure 1.2 shows the effect of the grid spacers on the heat transfer coefficient at 80 seconds after the reflood initiation. The heat transfer coefficient downstream of the grid spacers tends to be higher than that upstream of the spacers. Figure 1.3 shows the turnaround and quench temperatures at various elevations in the core. The location of the grid spacers are shown in the figure. The turnaround and the quench temperatures downstream the grid spacer tend to be lower than that upstream the spacer.

This effect can be called a heat transfer enhancement due to the grid spacers. There may be several factors which affect the heat transfer and hence determine the turnaround temperature during reflood. In a case of a typical PWR with a cold leg injection, major factors for the evaluation of the turnaround temperature will be the local power distribution, the location of the quench front, and the existence of the grid spacers for a given core inlet boundary condition.

Figure 1.4 shows the results of the fuel balooning experiment at West Germany (KFK)[5]. As shown in the figure, the balooning ratio is strongly affected by the power distribution and the location of the grid spacers. The local power distribution will be dominant, as the

maximum temperature is the direct results of the high initial temperature and the high local power. The flow pattern above the quench front is generally different from that below the quench front in the core. Also the heat transfer coefficient above the quench front is gradually decreasing with the distance from the quench front during the reflood transient[3]. Although the effect of the grid spacers may be the least of the three, it will shift the location of the hottest spot in the downstream region and it will decrease the maximum clad temperature.

The effect of the grid spacers on the heat transfer is thus favorable for the safety margin of the fuel rods in the reflood phase, however, it has not been studied in detail. FLECHT bundle reflood experiment has shown that the heat transfer is enhanced by the spacers when the flooding rate is higher than 3.8 cm/seconds[6]. Yao et al.[7] has discussed the heat transfer mechanisms and has proposed the model based on the single phase flow conditions. FEBA experiment[8] in West Germany has shown the heat transfer enahncement by the spacers. However, the heat transfer mechanisms and the flow regime have not been clearly identified.

JAERI is planning to conduct the Series-8 small reflood experiment, and the effect of the grid spacers on the heat transfer will be investigated as a part of the test series. The mechanisms and the quantification of the heat transfer enhancement will also be investigated. Described in Appendix is a plan of the grid spacer effect experiment. The modeling of the grid spacer effect on the heat transfer enhancement will be necessary for the best-estimate reflood analysis code[9].

According to the results of the CCTF (Cylindrical Core Test Facility) experiments at JAERI[10], the core thermo-hydraulics were sometimes different from the results of FLECHT or PKL reflood experiments. It also showed the larger safety margin exists in CCTF than the current evaluation model calculation. The effect of the grid spacers on the core thermo-hydraulics will be important for the analytical and the experimental coupling of the test results.

1.2 Objectives

The objectives of the present preliminary analysis of the grid spacer effects are as follows:

(1) to review the existent experimental data concerning the heat

transfer enhancement,

(2) to review the previous analytical models, and

(3) to describe the present heat transfer model.

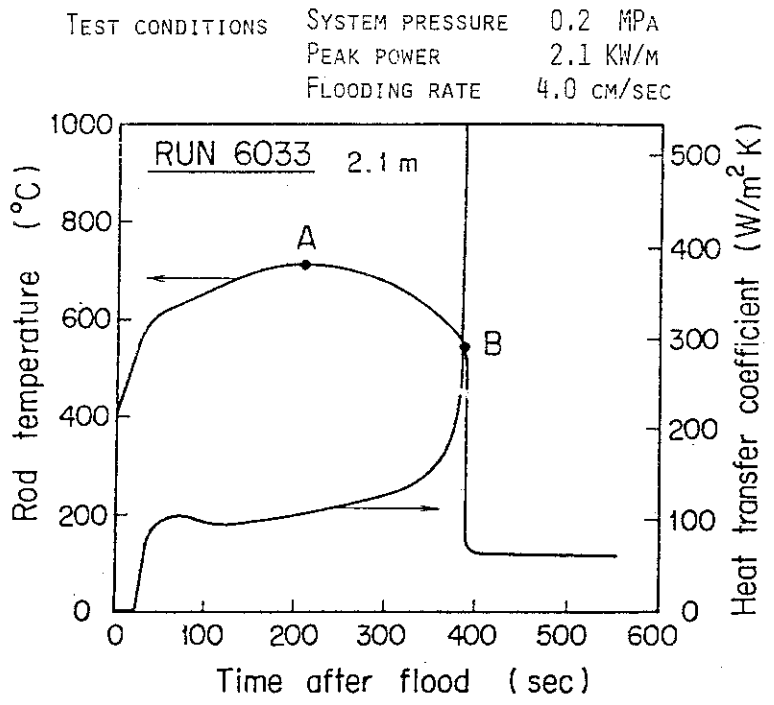

Figure 1.1 Temperature and the heat transfer responses during reflood phase

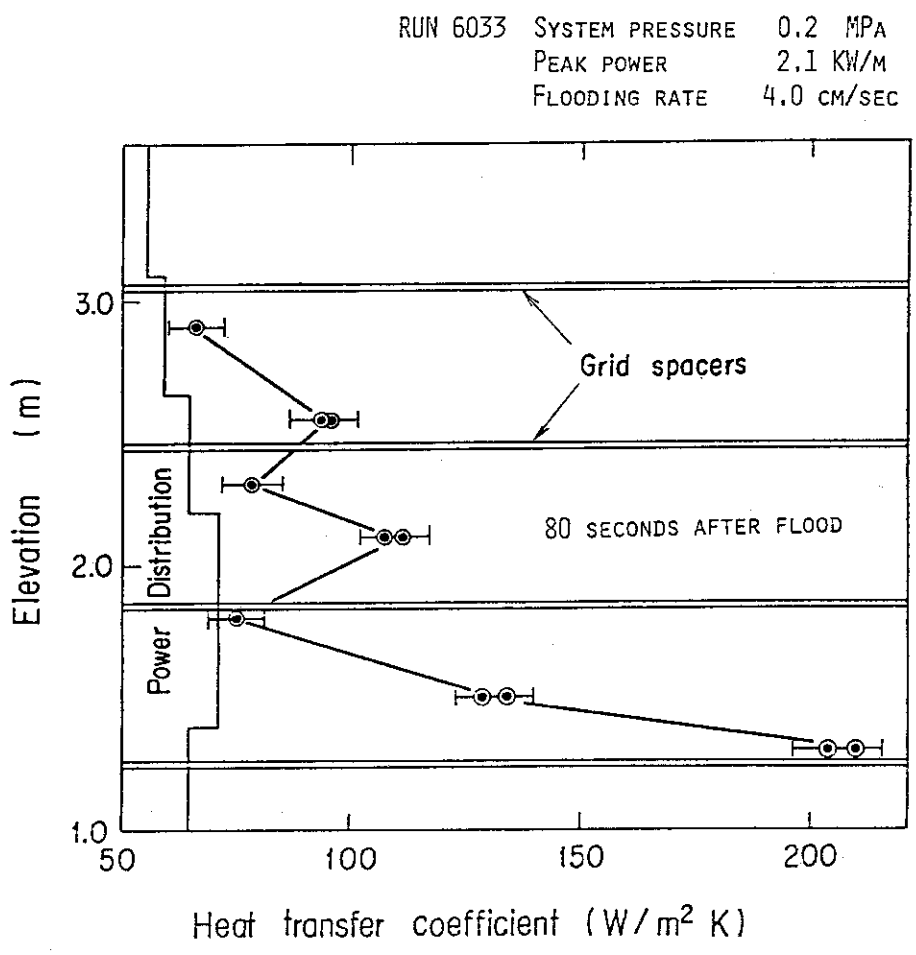

Figure 1.2 Distribution of heat transfer coefficient at JAERI's experiment

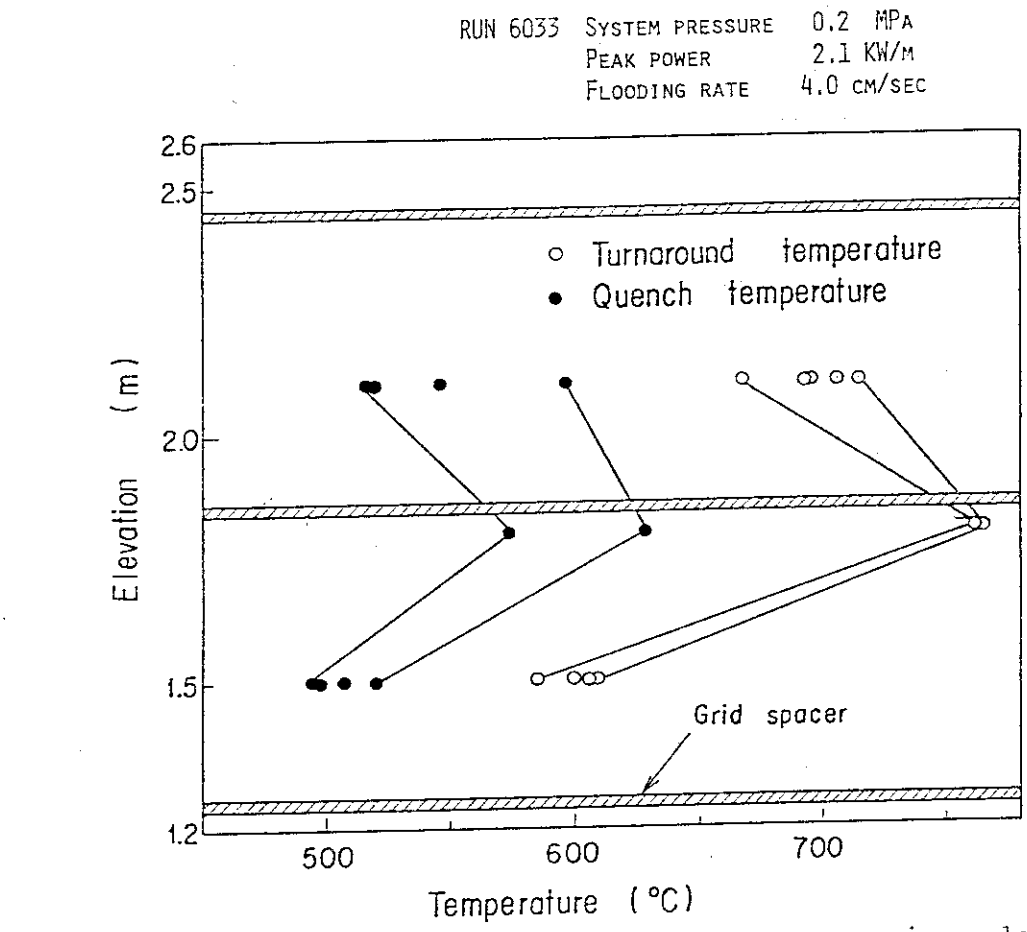

Figure 1.3 Turnaround and quench temperature at various elevations of the same power at JAERI's experiment

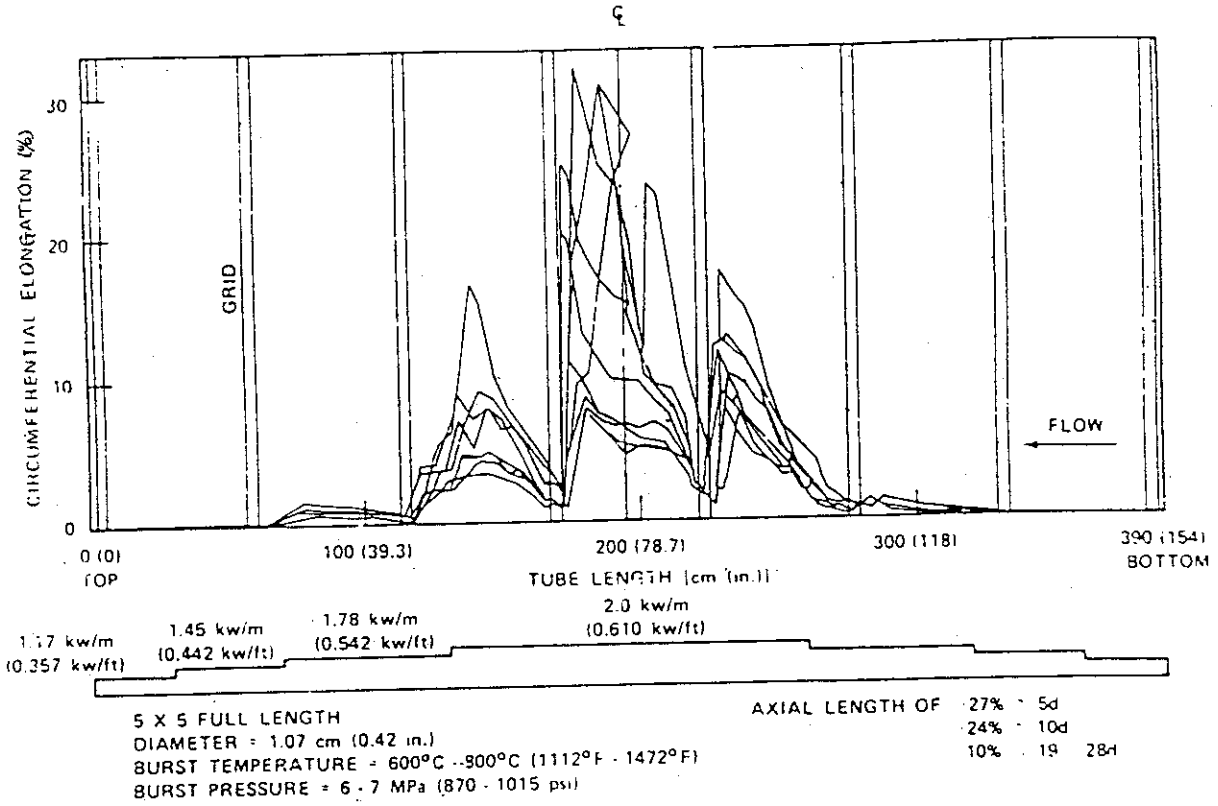

Figure 1.4 German Out-of-Pile test results

2. Effect of the Grid Spacers on the Heat Transfer

The bundle reflood experiments indicated that the heat transfer enhancements were observed at the region downstream the grid spacers. The heat transfer mechanisms near the grid spacer are not clearly identified, and the experimental data with detailed information are rare up to now. First we will review the existing experimental data about the heat transfer enhancement near the grid spacers, and then we will review the analytical models in the following sections.

2.1 Review of the Experiments

2.1.1 FLECHT

FLECHT (Full Length Emergency Core Heat Transfer) consists of several series of experiments. The experiments were conducted under the forced and the gravity feed injection conditions. The simulated core consisted of 105 heated rods in FLECHT Low Flooding[11] and Skewed Core experiments[12].

Figure 2.1 shows the measured data for the quench front movement obtained in Skewed Core Run 11003. Also shown is the skewed core power distribution in the figure. Quench front seems to move quite smooth regardless of the existence of the grid spacers.

The heat transfer coefficients are shown in Fig.2.2. The heat transfer coefficient reached a stationary value at time t_1 (~30 seconds) as indicated in the figure. This corresponds to the beginning of the liquid effluent from the core exit and to the time of the stationary value of the void fraction as shown in Fig.2.3. This means that the two-phase flow was established at about 30 seconds. The heat transfer coefficient at 3.20 m elevation is generally higher than that at 2.05 or at 3.35 m elevation. This indicates that the heat transfer above the grid spacer is enhanced by the grid spacer and its effect decreases with the distance from the grid spacer.

The distributions of the heat transfer coefficient and the void fraction in the core are shown in Figs.2.4 and 2.5, respectively. The heat transfer enhancement due to grid spacers, which is the difference of the heat transfer coefficient below and above the spacer, can be observed in the upper part of the core. This augmentation effect seems to be dominant when the quench front, shown in Fig.2.1, is far

from the grid spacer. The void fraction in the upper part of the core, which contains the spacer in the differential pressure measurement section, is lower than that without it. Although the frictional pressure loss at the grid spacers may not be negligible, this implies the existence of more water droplets suspending near the spacers.

Figure 2.6 shows the effect of the test conditions on the heat transfer distributions at the time when the two-phase flow was first established along the while core. The test condition are summarized in Table 2.1. The order of the heat transfer enhancement due to the grid spacers falls on the range of 10 to 100 $W/m^2 \cdot K$. The heat transfer augmentation is larger for the case of either the higher flooding rate, the lower system pressure, or the higher peak power.

2.1.2 FEBA

FEBA (Flooding Experiments with Blocked Arrays)[8] experiment in West Germany has been conducted to investigate the flow blockage characteristics during reflood. Test section consists of 5×5 electrically heated rods. To examine first the effect of the grid spacers, they conducted the reflood test with and without the grid spacer at midplane. Figure 2.7 shows the schematic of the test bundles.

Figure 2.8 shows the experimental results of the effect of the grid spacer at midplane on the heater rod surface temperature upstream and downstream of the grid spacer. One experiment was done with a grid spacer at midplane and the other was done without it. Comparing with both experiments, the heat transfer enhancement due to the grid spacer can only be observed downstream of the grid spacer. The temperature decrease due to the grid spacer is about 100°C at the most.

FEBA was the only experiment that has tried to investigate the effect of the grid spacers directly, however, the heat transfer mechanisms near the grid spacer based on the flow observation have not been reported.

2.1.3 JAERI's Small Reflood Experiment

JAERI has conducted several series of reflood experiments in the small scale reflood facility[4][13][14] to investigate the reflood phenomena. The test section bundle consisted of full length 4×4 electrically heated rods from Series 1 through Series 6 experiments.

JAERI has also been conducting Large Scale Reflood Test Program with almost 2,000 heated rods to demonstrate the effectiveness of the emergency core cooling system during reflood. However, only the results of the small scale reflood test are described here.

Figure 2.9 shows the heat transfer data at various elevations obtained in JAERI Run 6033. Test conditions of JAERI experiments are summarized in Table 2.2. The two-phase flow was established at about 60 seconds when the heat transfer coefficients along the core reached some stationary values as indicated by t_1 in Fig.2.9. Heat transfer coefficients are higher for 2.1 and 2.55 m elevations enhanced by the grid spacers as shown in Fig.2.9.

Figure 2.10 shows the effect of the test conditions on the heat transfer coefficient distribution when the two-phase is first developed along the core. The test conditions are summarized in Table 2.2. The locations of the grid spacers are also shown in the figure. The heat transfer enhancement due to the grid spacer tends to be larger for the case of the lower system pressure or the higher peak power.

The effect of the flooding rate on the heat transfer augmentation is not so dominant as that in FLECHT experiment shown in Fig.2.6, since the flooding rate varies a little in JAERI's experiment. It should also be noted that the initial peak clad temperature of FLECHT (~870°C) is much higher than that of JAERI's experiments (~400°C). The high wall temperature in FLECHT may not enable the water droplets to contact the wall easily, resulting in the dispersed flow with large amounts of droplets in the upper part of the core when the flooding rate is high.

2.2 Previous Models

2.2.1 Heat Transfer Mechanisms

Several models have been proposed on the mechanisms of the heat transfer enhancement near the grid spacers in the two-phase flow during reflood phase. The following heat transfer mechanisms have currently been classified[6][7].

(1) Atomization of the droplets

The flowing droplets in the dispersed flow region downstream the quench front will hit the edge of the spacers causing the atomization of the droplets. The increased number of droplets and the increased interfacial area will then cause the desuperheat of the vapor resulting

in the heat transfer enhancement from the wall to the vapor.

(2) Contact heat transfer

The droplets splashed and disturbed by the grid spacers may bounce to the hot wall to cause the direct contact heat transfer from the wall to the droplets.

(3) Acceleration

The vapor flow will be locally accelerated by the grid spacers due to the reduction of the flow area. The flow acceleration increases the local vapor velocity near the grid spacers, which enhances the local heat transfer.

(4) Radiation to the grid spacers

The grid spacers are commonly made of materials of a low heat capacity and they can easily be rewetted by impinging water droplets in a dispersed flow. After the rewetting of the grid spacers, the radiation heat transfer from the wall to the grid spacers would not be negligible in the vicinity of the grid spacers when the wall temperature is relatively high.

(5) Fin cooling

The spacers sometimes contact with the rods at the top of small dimples made on the side wall of the spacers to hold the rod bundles. Then the spacer itself may act as a cooling fin to the rod. The temperature of the grid spacers can be saturation temperature when the spacers are rewetted by the droplets in the dispersed flow.

(6) Disturbance

The two-phase flow will be mixed and disturbed by the spacer structure. The velocity and thermal fields will be affected by the spacers to cause a more uniform flow in the spacer region. The hydrodynamic and thermal boundary layers begin to reestablish their fully developed flows in the downstream of the spacers. The heat transfer in this region will be enhanced by the disturbed boundary layer.

2.2.2 Heat Transfer Correlations

Marek and Reheme[16] have proposed the correlation of the heat transfer enhancement at the grid spacers in the single phase flow in the form,

$$\frac{Nu}{Nu_0} = 1 + 5.55\ \varepsilon^2 \quad , \tag{1}$$

where Nu and Nu_0 denote the local Nusselt number with and without the spacer respectively, and ε is the blockage ratio of the spacer to the flow area. Equation (1) was derived from the analogy between the frictional pressure drop and the heat transfer from the wall at the spacers.

Based on the several experimental data of the heat transfer enhancement downstream of the grid spacers in the single phase flow, Yao et al.[7] developed a correlation for Reynolds number higher than 10^4 on the basis of Eq.(1) as

$$\frac{Nu}{Nu_0} = 1 + 5.55\,\varepsilon^2\, e^{-0.13(x/D)} \quad , \tag{2}$$

where x is the distance from the downstream end of the spacer and D is the hydraulic diameter of the flow channel.

Equation (2) implies the heat transfer is affected by the spacer in the region about ten times the length of the hydraulic diameter in a single phase flow.

In the post CHF reflood phase condition, Yao et al.[7] has developed the heat transfer model which contains the disturbance, the radiation, and the fin cooling mechanisms described in Section 2.2.
The mechanism of the atomization or the coupling of the droplets, which might be characteristic features in the reflood conditions, were not included in their modeling. The total heat flux qw has been written in the form:

$$qw = qw,rad + qw,fin + qw,dis \quad , \tag{3}$$

where subscript rad, fin and dis denote the radiation, fin cooling, and two-phase flow disturbance, respectively.

The "qw,rad" is estimated by the radiation from the wall to the rewetted spacer. The fin cooling is localized at the spacers assuming the conservative fin cooling of the hot wall. Equation (2) is utilized to evaluate the disturbance term "qw,dis" assuming the homogeneous vapor flow.

Table 2.1 Test conditions of FLECHT Skewed Core experiment

Symbol	FLECHT Run No.	System Pressure (MPa)	Peak Power (KW/m)	Flooding Rate (cm/sec)	Coolant Temp. (°C)	Time Taken for Fig.2.6 (sec)
◉	11003	0.28	2.3	2.5	53	30
○	13609	0.14	2.3	2.5	31	30
×	13711	0.41	2.3	2.5	67	30
△	11618	0.28	1.5	3.8	52	20
□	16022	0.28	3.3	3.8	53	20
◎	12102	0.28	2.3	7.6	52	20
●	13001	0.28	2.3	14.5	52	12.5

Other conditions:

Initial Peak Clad Temperature : 871°C

Table 2.2 Test conditions of JAERI small reflood experiment

Symbol	Run No.	System Pressure (MPa)	Peak Power (KW/m)	Flooding Rate (cm/s)	Coolant Temp. (°C)	Time taken for Fig.2.10 (sec)
◉	6033	0.2	2.0	4	100	60
○	6012	0.1	2.0	4	85	60
×	6021	0.4	2.0	4	120	60
△	6039	0.2	1.6	4	100	60
□	6028	0.2	2.8	4	100	50
●	6047	0.2	2.0	7.5	100	30

Other conditions:

Initial Peck Clad Temperature : 400°C

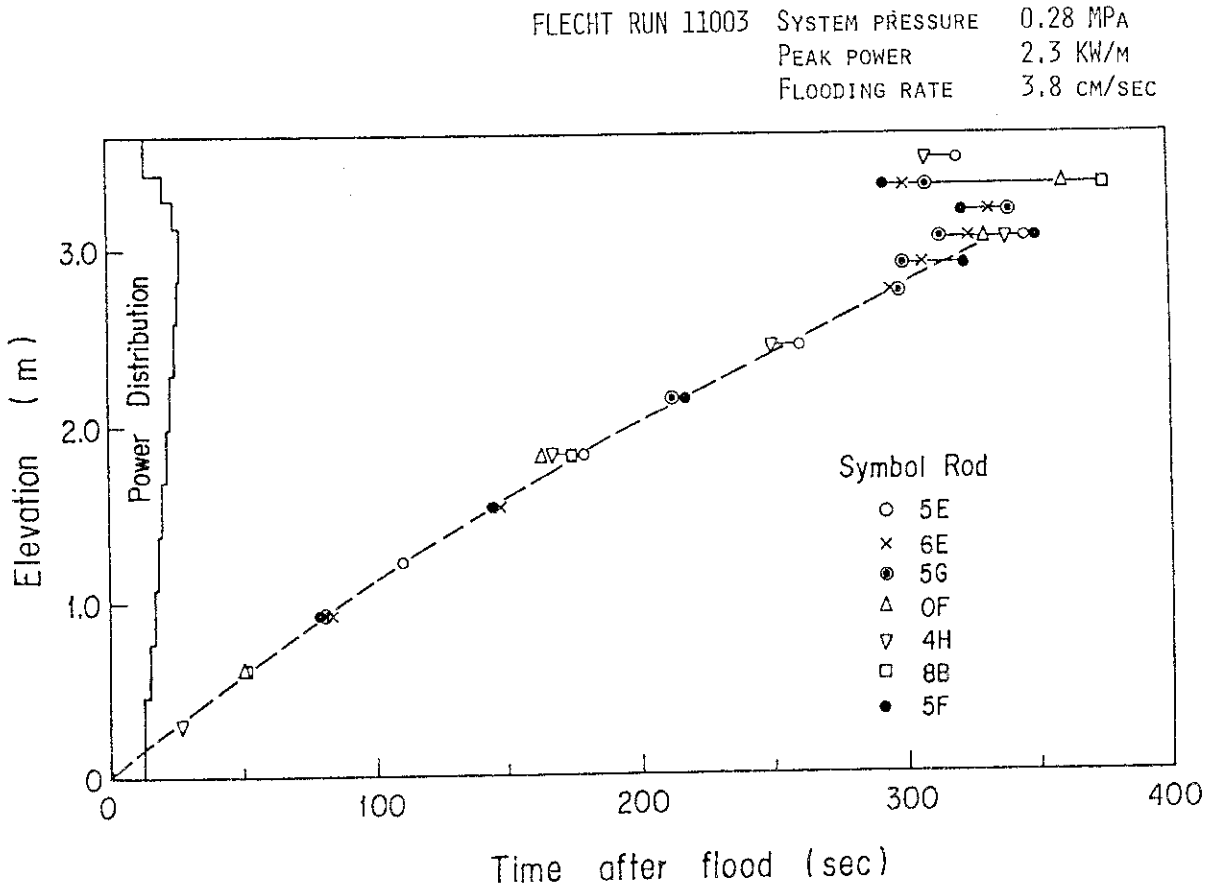

Figure 2.1 Quench front movement in FLECHT Skewed Core experiment

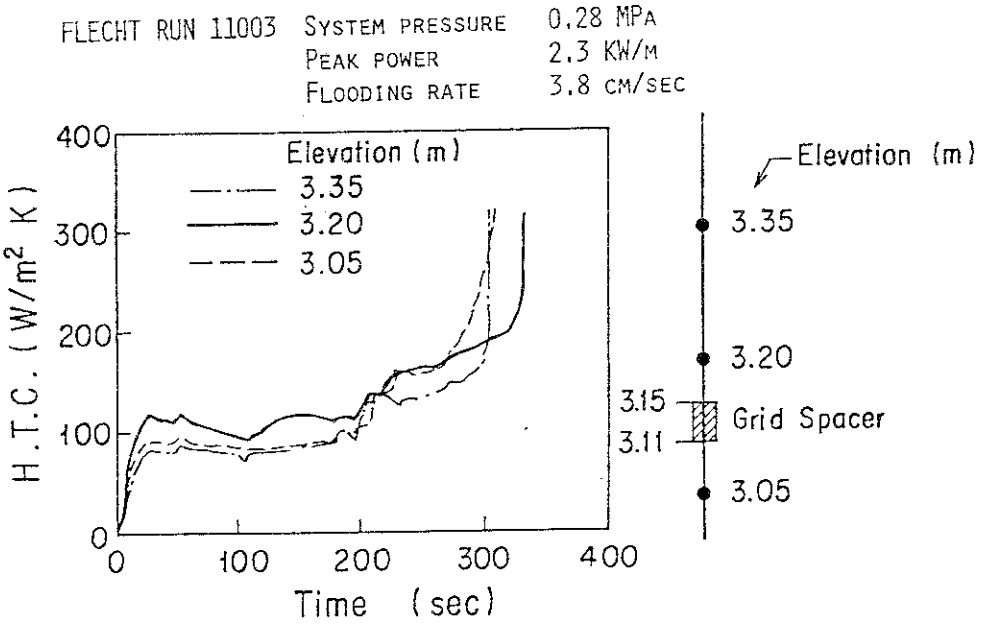

Figure 2.2 Heat transfer coefficients near the grid spacer

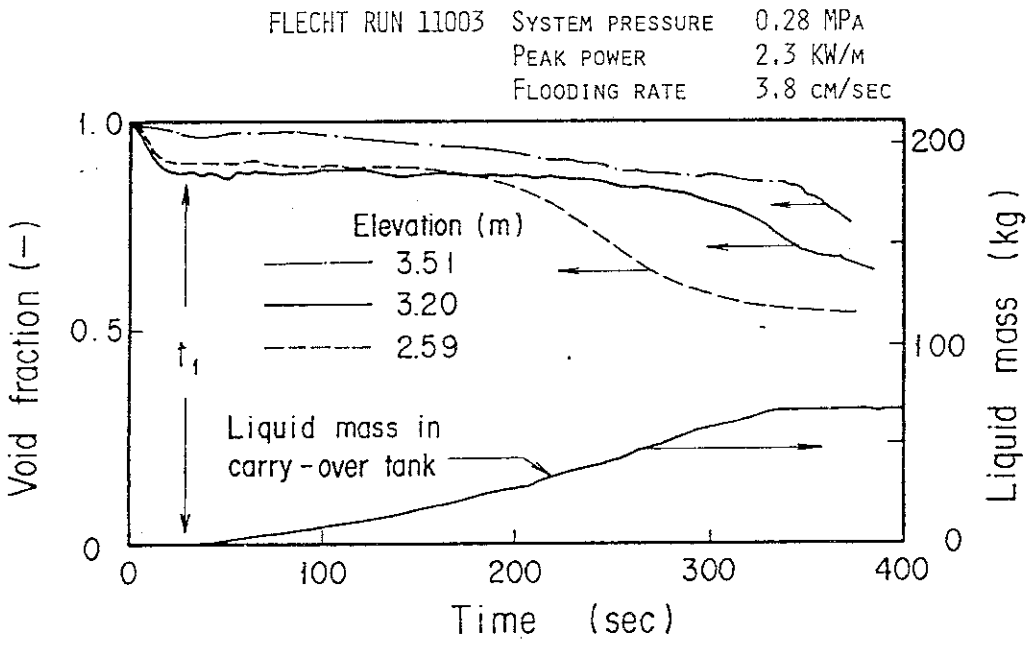

Figure 2.3 Void fraction and carried over liquid mass

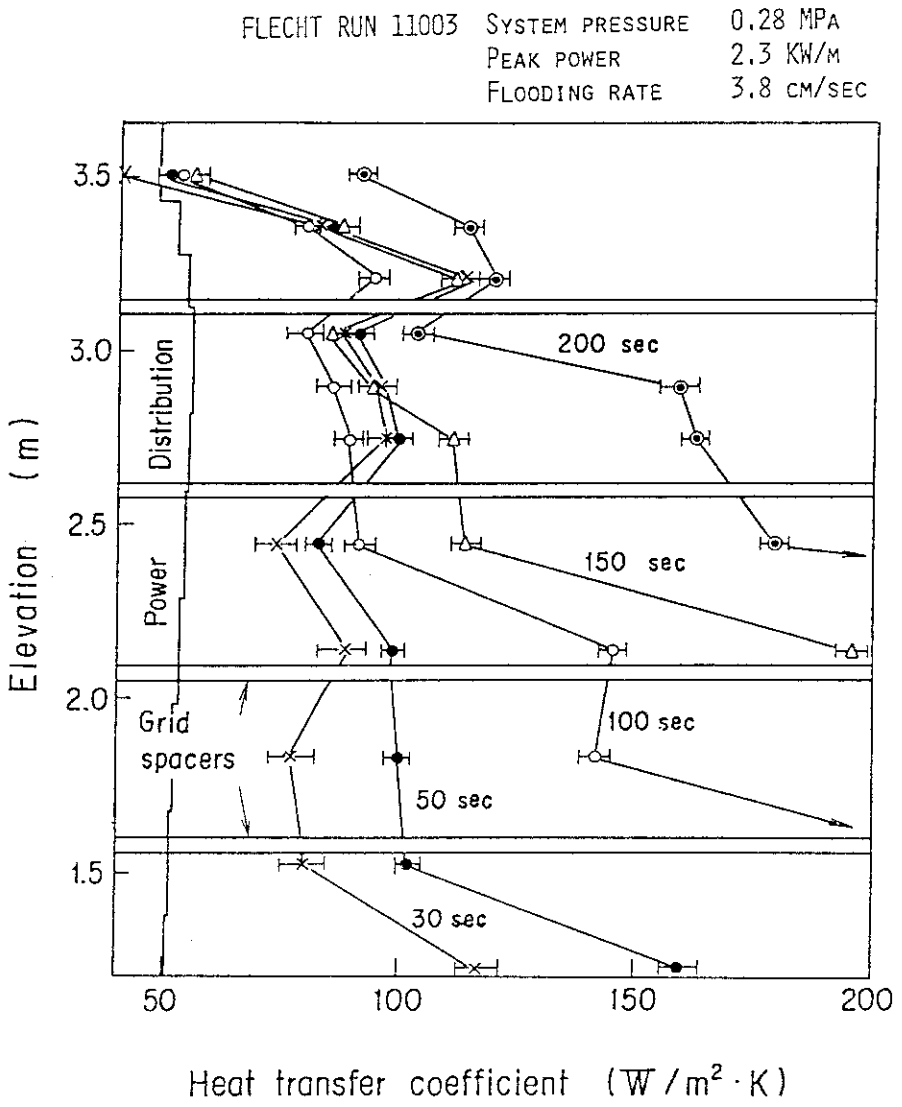

Figure 2.4 Axial distribution of heat transfer coefficients

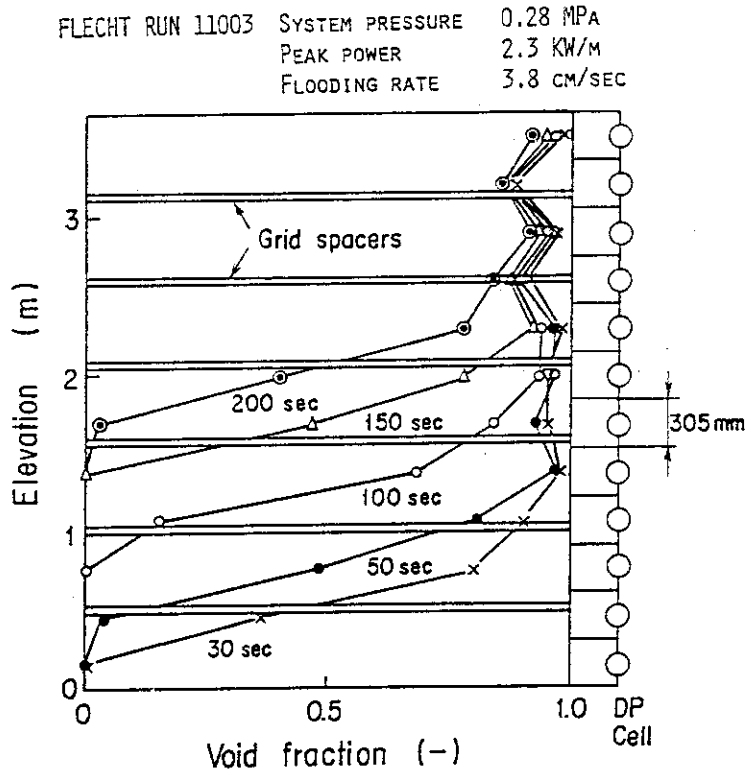

Figure 2.5 Axial distribution of void fraction

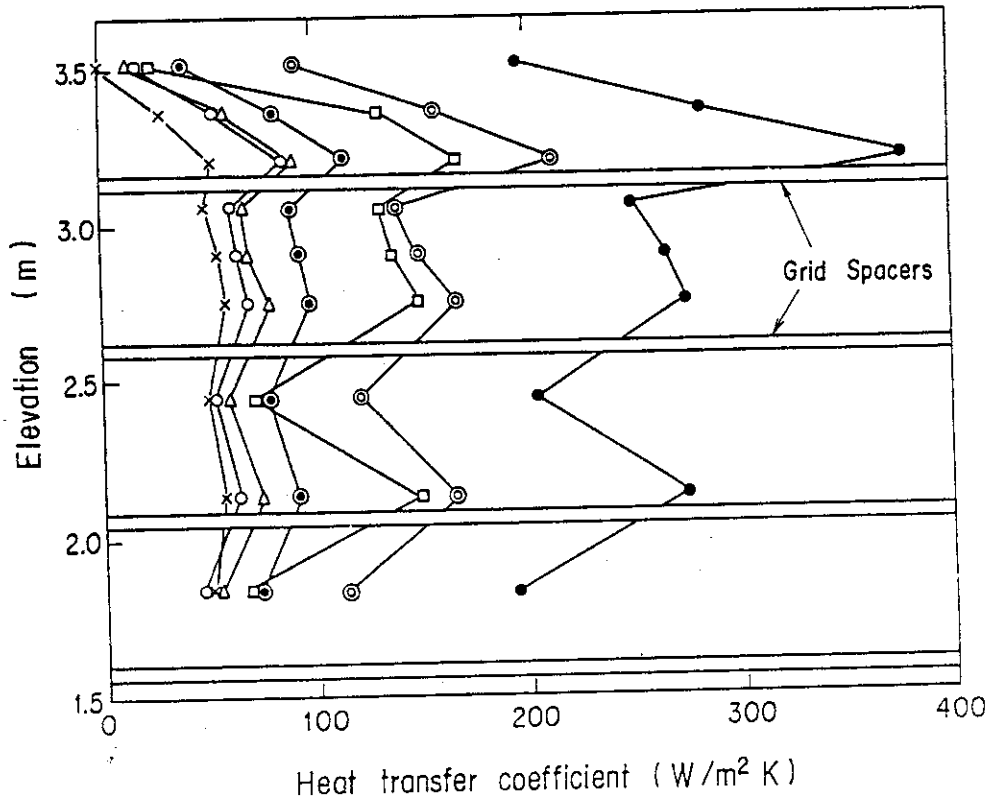

Figure 2.6 Effect of test conditions on the axial heat transfer distribution (FLECHT)

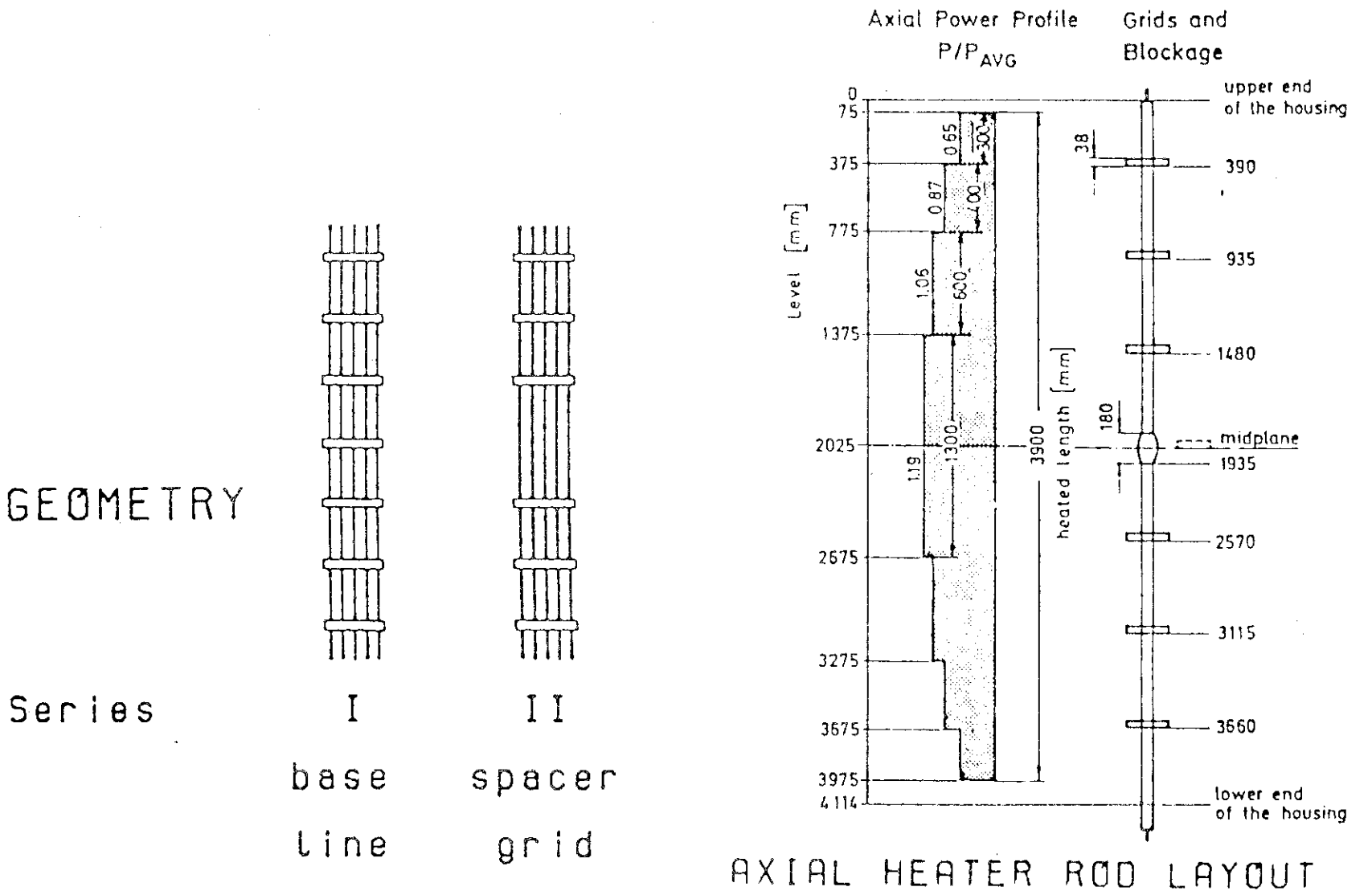

Figure 2.7 Schematic of FEBA test bundles

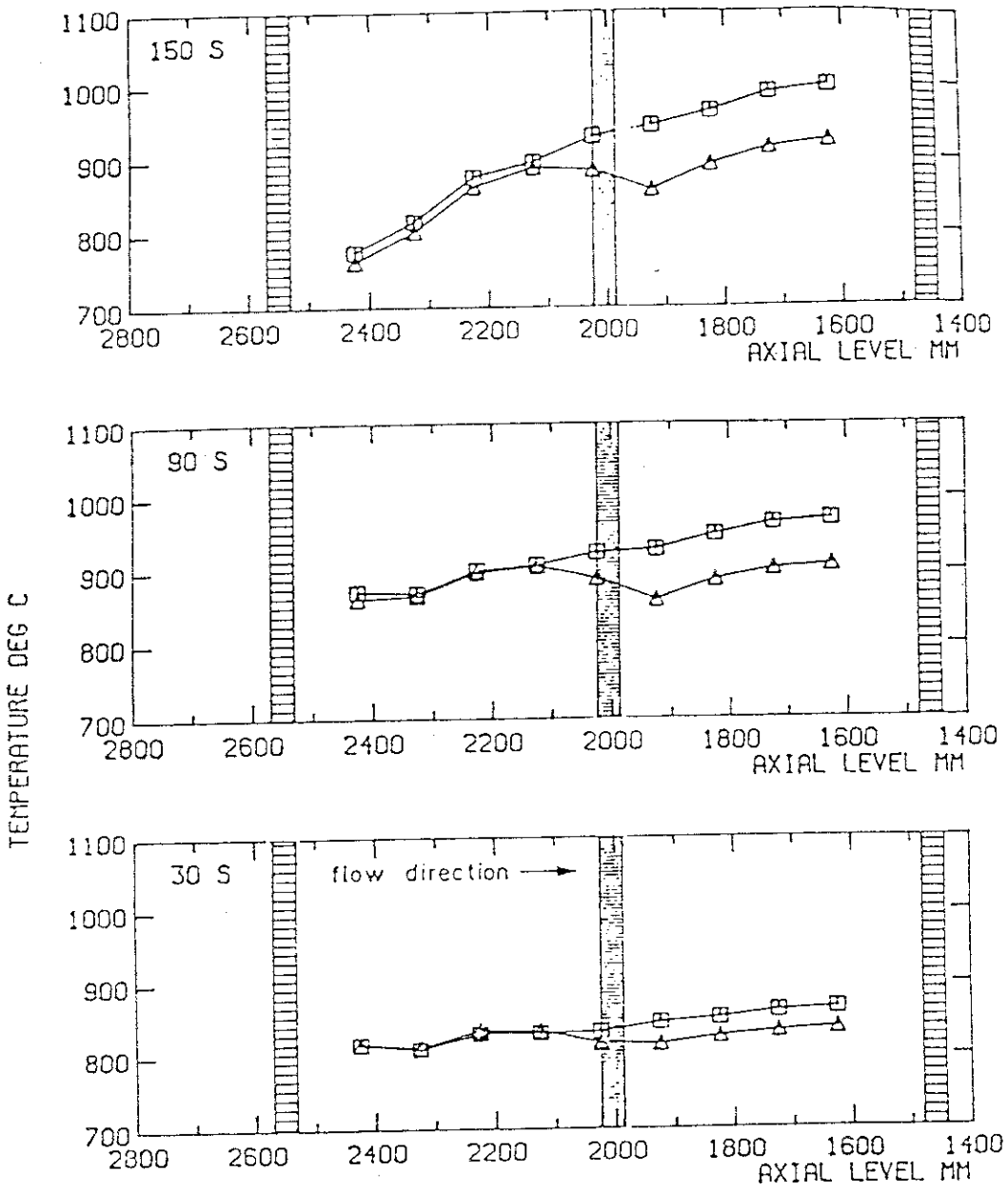

flood parameters: v = 3.4 cm/s, p = 2.0 bar

△ test 223, (with spacer grid at midplane)
□ test 234, (without spacer grid at midplane)

Figure 2.8 Influence of a grid spacer on the axial temperature profile

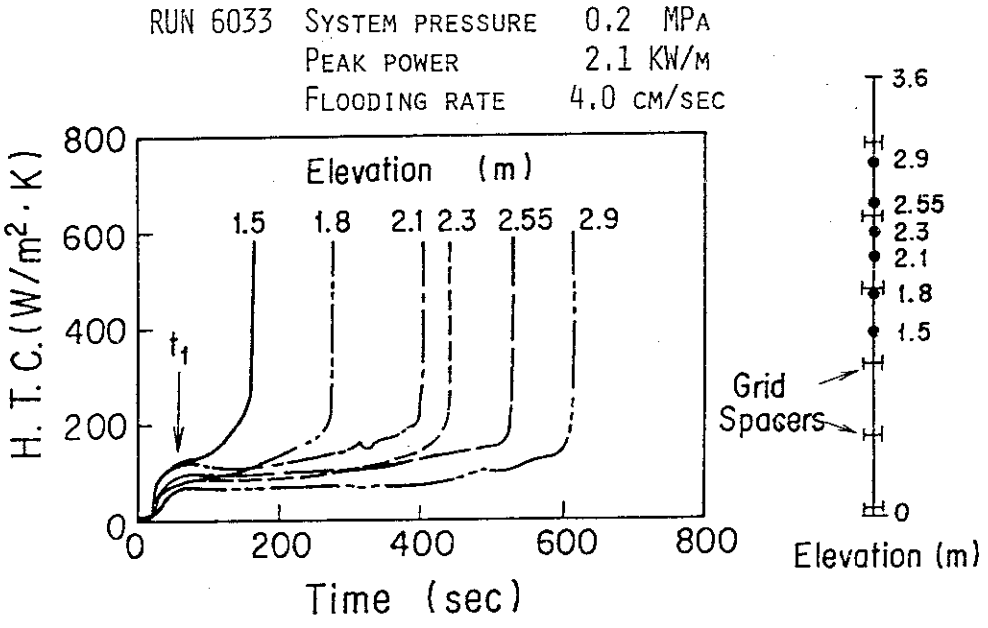

Figure 2.9 Heat transfer coefficient near the grid spacers

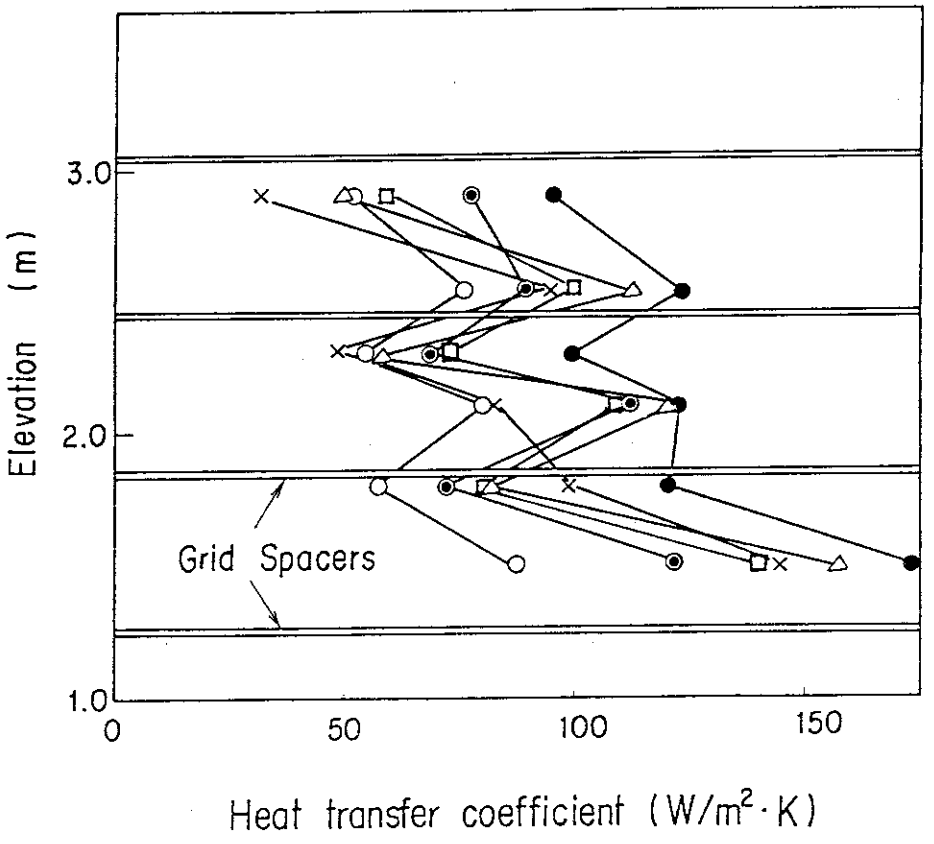

Figure 2.10 Effect of test conditions on the axial heat transfer distribution (JAERI)

3. Preliminary Analysis

3.1 Discussion on the Previous Models

In a single phase flow, the effect of the disturbance or the mixing will be dominant on the heat transfer enhancement due to the spacers. In a reflood two-phase flow, however, the situation is rather complicated because of the existence of the water droplets in the flow channel.

The contact heat transfer between the droplets and the wall has been studied by Iloeje et al.[15] and found to be generally small in magnitude. The effect of the fin cooling will not be large, since the pinpoint contact area between the rod and the spacer will be so small to give a good heat conduction to the spacers.

The effect of the flow acceleration will be limited to the vicinity of the spacers, and the heat transfer dependence on the velocity change is rather weak for the most blockage ratios of the spacers if we assume a Dittus-Boelter type equation:

$$Nu \sim V^{0.8} \quad ,$$

where Nu is the Nusselt number and V is the vapor velocity.

Radiation to the spacers may not be negligible when the wall temperature is high and the spacer is rewetted. This effect can be accurately treated by the radiation law, therefore the information needed is the time when the rewetting of the spacers occurs.

Besides the effect of the atomization of the droplets, we should consider the mechanism of the coalescence or the uniting of the droplets. Some of the disturbed droplets by the spacers may couple to each other to increase the size of droplets downstream of the spacers. The small droplets will be carried over to the exit of the core due to the velocity acceleration near the spacers. On the other hand, the large droplets tend to remain just above the spacers due to their large gravity force compared with the drag force of the vapor flow. Sometimes when the flooding rate is relatively high, the flow just above the grid spacers may be more like film boiling than the dispersed flow due to the coalescence of the droplets as illustrated in Fig.3.1. The large amount of water above the spacer will cause the heat transfer enhancement. This situation of the enhanced heat transfer with the

smaller void fraction at the spacers are indicated in FLECHT experiment as already shown in Figs.2.4 and 2.5. This mechanism might cause a multiple quench front propagation at the spacers when the amount of water above the spacers is excessively large.

The flow observation near the grid spacers will supply the information about the flow pattern. The main heat transfer mechanism at the spacers, which may depend on the flow conditions, could be identified by the droplets movement or the droplets diameter distribution near the spacers.

3.2 Present Model

In order to clarify the heat transfer enhancement mechanism of the grid spacers, we need detailed information near the grid spacers. The flow observation near the grid spacers will be most valuable to determine the flow pattern which may affect the heat transfer enhance-enhancement. The vapor superheat temperature and the rewetting time of the grid spacers will be utilized to evaluate the radiation heat transfer from the wall.

In the present preliminary analysis, the heat transfer correlation developed by Murao and Sugimoto[3] will be adopted as a guide to evaluate a local heat transfer enhancement by the grid spacers, assuming the flow situation of the coalescence of the droplets described in the previous section. The correlation is

$$h = h_{sat} + h_R \quad , \tag{4}$$

where

$$h_{sat} = 0.94(1-\alpha)^{\frac{1}{4}} \left[\frac{\lambda_g^{\,3} \rho_g (\rho_\ell - \rho_g) H_{fg}}{L_q \mu_q \Delta T_{sat}} \right]^{\frac{1}{4}} \quad ,$$

$$h_R = E\sigma(1-\alpha)^{\frac{1}{2}} \frac{T_w^{\,4} - T_{sat}^{\,4}}{\Delta T_{sat}} \quad .$$

The first term, h_{sat}, of the right hand side of Eq.(4) is similar to the Bromly type film boiling correlation, however, it is modified by the void fraction α and the distance from the quench front L_q. The radiative heat transfer is described in the second term, h_R, modified by the factor $(1-\alpha)^{\frac{1}{2}}$ accounting for the existence of the

liquid in the flow channel.

The correlation (4) was valid for the saturated film boiling region rather than the dispersed flow region, and the error predicted by Eq.(4) was about ±20% for JAERI's small scale reflood experiment and FLECHT Low Flooding experiment except for the vicinity of the spacers.[3]

Figure 3.2 shows the example of the comparison of the measured heat transfer coefficient obtained at JAERI's experiments and the calculated heat transfer coefficient based on Eq.(4). Figure 3.3 shows the measured and the calculated heat transfer distributions at 60 seconds after flood. Equation (4) gives fairly good estimation of the heat transfer coefficient as an average when the two-phase flow is first established along the core. The quench front is about 1.0 m above the bottom of the core at that time. Also shown in the figure is the heat transfer coefficient calculated by Eq.(3). Nu_0 in Eq.(2) is evaluated by the Dittus－Boelter's equation assuming the vapor temperature as the average of the wall and saturated temperatures. The vapor velocity is evaluated by the quench front velocity, the steam generation rate in the quenched region and the local void fraction. A fairly large difference between the calculations by Eqs.(3) and (4) may be due to the difference of the assumed flow patterns.

To eliminate the effect of the temperature difference caused by the initial temperature and the axial power distribution, radiative heat transfer term, h_R, can be subtracted from the equation (4),

$$h_{sat} = h - h_R \quad , \tag{5}$$

as the other term, h_{sat}, is a very weak function of the wall temperature.

Figure 3.4 shows the comparison of the measured and the calculated heat transfer coefficients, h_{sat}, as a function of the distance from the grid spacer for JAERI and FLECHT Skewed Core experiments. The data are taken at the highest power region. The radiative term is subtracted by equations (4) and (5). The h_{sat} of JAERI's data are higher than that of FLECHT data due to the lower void fraction.

To compare the heat transfer coefficient, h_{sat}, between two facilities regardless of the void fraction difference, the following correction factor B(x) is introduced tentatively:

$$h_{sat,meas} = h_{sat,calc} \times B(x) \quad ,$$

where meas and calc denote the measured and calculated, respectively,

and x is the distance from the upper edge of the grid spacer.

Figure 3.5 shows the plot of the correction factor, B(x), for several experiments at JAERI and FLECHT Skewed Core. The data are taken in the region above the grid spacer at the highest local power distribution, and the times of the data taken are the same as in Table 2.1 and 2.2. The relationship of B(x) with the distance x can be simply correlated by

$$B(x) = ax + b \quad , \tag{6}$$

where

$$\begin{aligned} a &= -2.0 \ (1/m) \quad , \\ b &= 1.7 \pm 0.3 \ (m) \ . \end{aligned} \tag{7}$$

It should be noted that the tentative correction factor (6) has been derived from the data at the beginning of the establishment of the two-phase flow. The heat transfer correlation (4) still holds for the most part of the transient, especially in the vicinity of the quench front as shown in Fig.3.2. Therefore, the correction factor (6) can be adopted when the quench front is far from the concerned location.

A more detailed heat transfer measurement along the axial direction near the grid spacer will be required to testify the functional relationship of the heat transfer enhancement by the grid spacers with the analytical models.

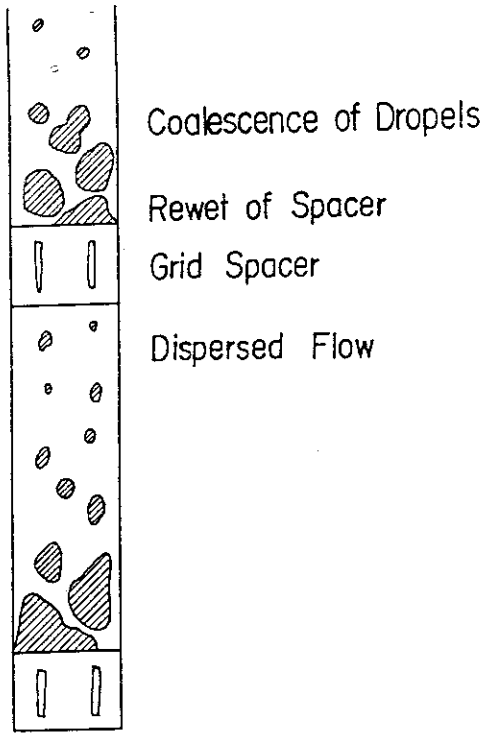

Figure 3.1 Coalescence of droplets downstream of the grid spacer

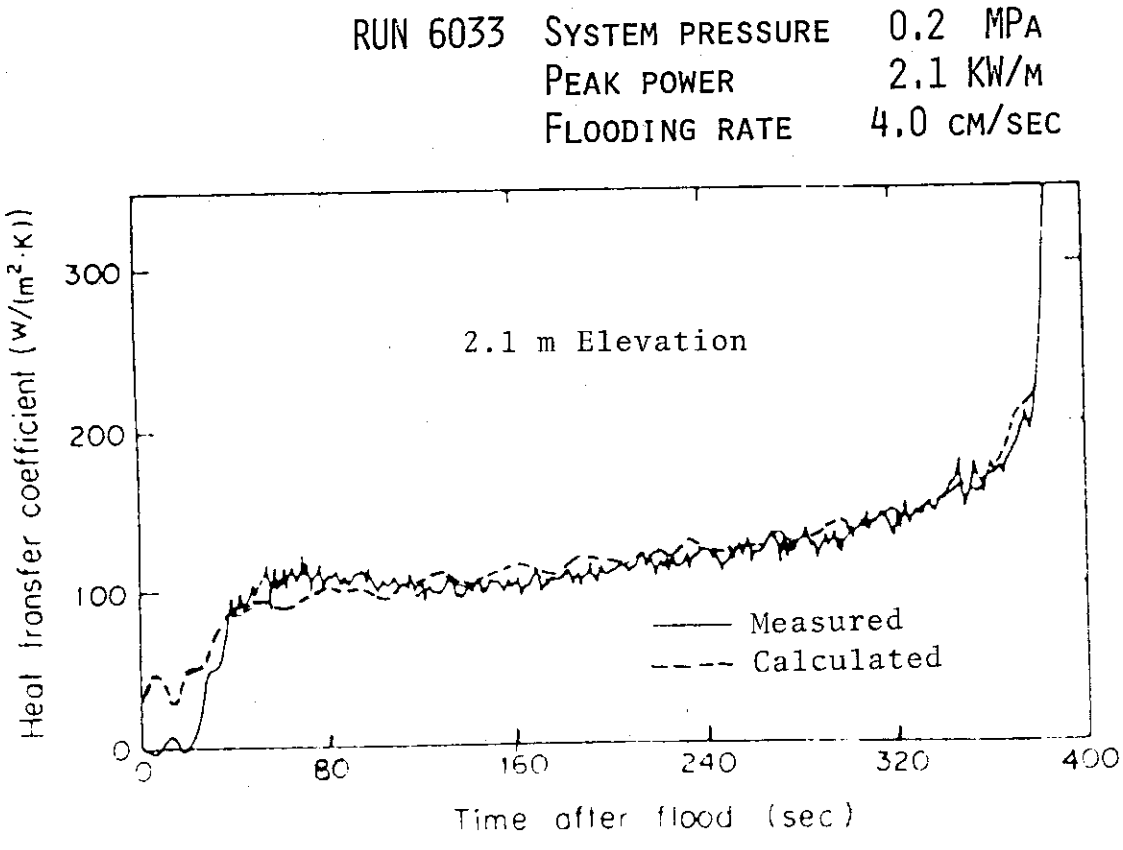

Figure 3.2 Measured and calculated heat transfer coefficient

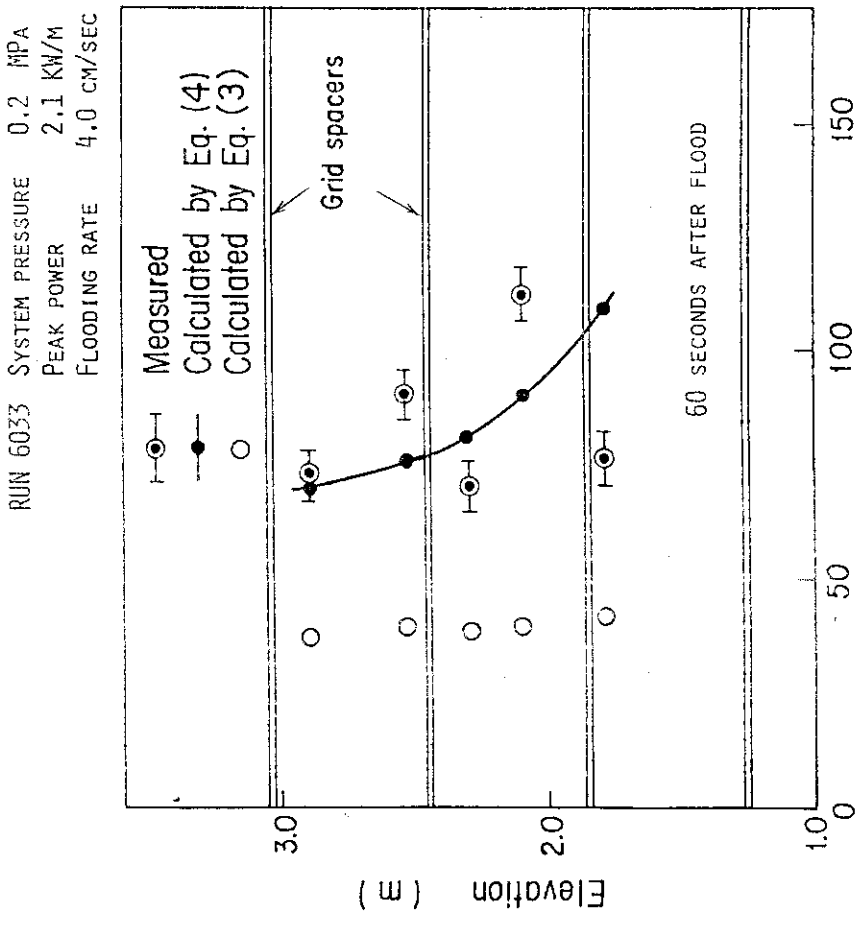

Figure 3.3 Measured and calculated heat transfer distribution

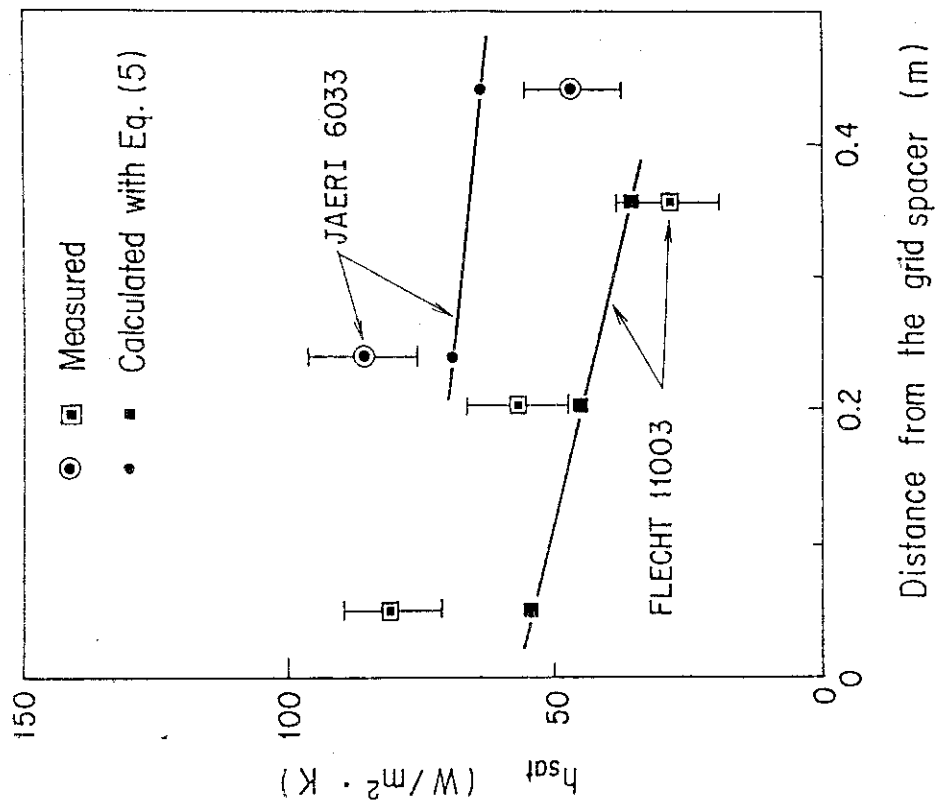

Figure 3.4 Measured and calculated saturated heat transfer coefficient

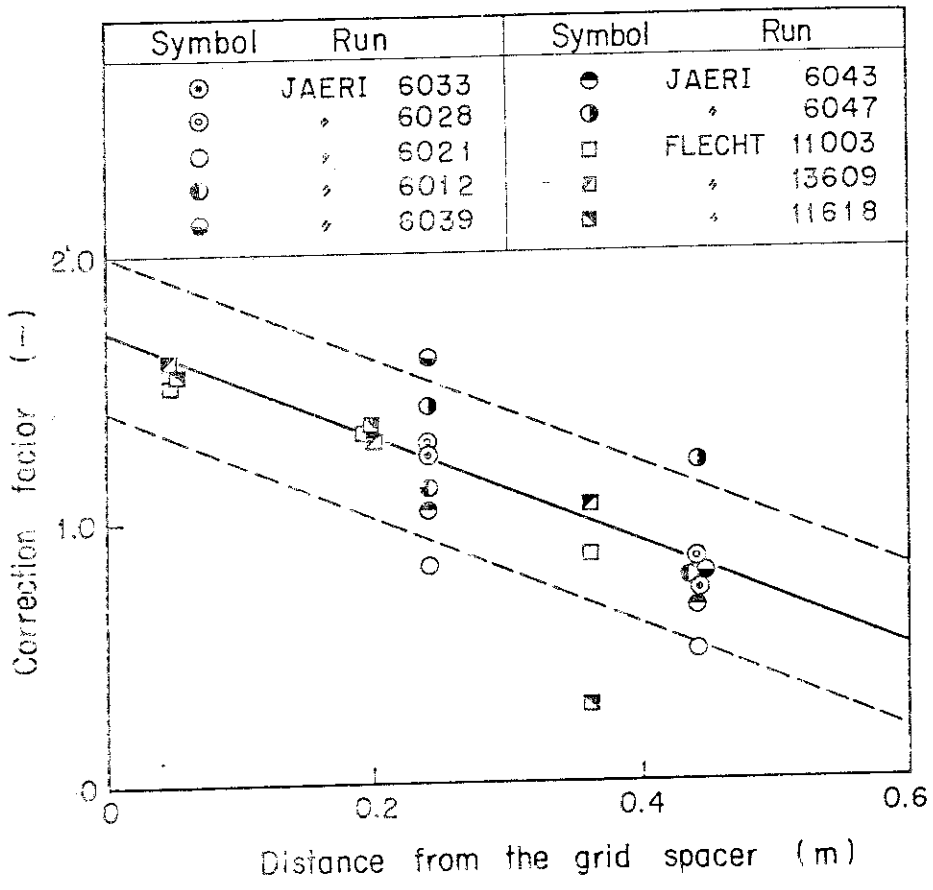

Figure 3.5 Heat transfer correction factor for JAERI and FLECHT experiment

4. Conclusions

(1) Reflood experiments at JAERI and other facilities were reviewed to quantify the heat transfer enhancement by the grid spacers. It was found that the heat transfer coefficient downstream the grid spacers was generally larger than that upstream the spacers. The heat transfer enhancement was clearly observed after the establishment of the two-phase flow along the core, and it decreased with the distance from the grid spacer.

(2) The previous models on the heat transfer enhancement by the grid spacers were reviewed and discussed. It was pointed out that the proposed heat transfer mechanism of the coalescence of the water droplets could be dominant over the previous models for certain flow conditions.

(3) To evaluate the effect of the grid spacers on the heat transfer enhancement, a tentative correction factor was obtained for the heat transfer correlation for the saturated film boiling developed by the authors. The corrected heat transfer coefficient agreeed well with the data during the first stage of the reflood transient.

Acknowledgment

The authors are much grateful to Dr. M. Nozawa, Dr. S. Katsuragi, Dr. M. Ishikawa and Dr. K. Hirano for their hearty suggestions and encouragement. The authors are also deeply indebted to Mr. T. Iguchi, Mr. T. Sudoh, Dr. H. Akimoto, Mr. T. Okubo, and Mr. Y. Niitsuma for their analytical and experimental supports.

4. Conclusions

(1) Reflood experiments at JAERI and other facilities were reviewed to quantify the heat transfer enhancement by the grid spacers. It was found that the heat transfer coefficient downstream the grid spacers was generally larger than that upstream the spacers. The heat transfer enhancement was clearly observed after the establishment of the two-phase flow along the core, and it decreased with the distance from the grid spacer.

(2) The previous models on the heat transfer enhancement by the grid spacers were reviewed and discussed. It was pointed out that the proposed heat transfer mechanism of the coalescence of the water droplets could be dominant over the previous models for certain flow conditions.

(3) To evaluate the effect of the grid spacers on the heat transfer enhancement, a tentative correction factor was obtained for the heat transfer correlation for the saturated film boiling developed by the authors. The corrected heat transfer coefficient agreeed well with the data during the first stage of the reflood transient.

Acknowledgment

The authors are much grateful to Dr. M. Nozawa, Dr. S. Katsuragi, Dr. M. Ishikawa and Dr. K. Hirano for their hearty suggestions and encouragement. The authors are also deeply indebted to Mr. T. Iguchi, Mr. T. Sudoh, Dr. H. Akimoto, Mr. T. Okubo, and Mr. Y. Niitsuma for their analytical and experimental supports.

References

1. Cadek, F.F. et al., "PWR-FLECHT Full Length Emergency Cooling Heat Transfer Final Report", WCAP-7665, (1971).
2. Cermak, J.O., et al., "PWR-Full Length Emergency Cooling Heat Transfer (FLECHT) Group 1 Test Report", WCAP-7435, (1970).
3. Murao, Y., and Sugimoto, J., "Correlation of Heat Transfer Coefficient for Saturated Film Boiling during Reflood Phase Prior to Quenching", J. Nucl. Sci. Technol., 18 [4], 275～284 (1981).
4. Sugimoto, J., et al.: JAERI-M 8169, (in Japanese), (1979).
5. Wiehr, K., et al., "Fuel Rod Behavior in the Refill and Flooding Phase of a Loss-of-Cooling Accident", CONF-771252-5, (1977).
6. Conway, C.E., et al., "PWR FLECHT Separate Effects and System Effects Tests (SEASET) Program Plan", NRC/EPRI/Westinghouse Report No.1, Dec. 1977.
7. Yao, S.C., et al., "Heat Transfer Augmentation in Rod Bundles Near Grid Spacers", ASME paper 80-WA/HI-62, (1980).
8. Ihle, P., "FEBA Recent Results & Future Plans", presented at Eighth Water Reactor Safety Research Information Meeting, Oct. (1980).
9. Murao, Y., "Analytical Study of Thermo-Hydrodynamics Behavior of Reflood-Phase during LOCA", J. Nucl. Sci. Technol., 16 [11], (1979).
10. Murao, Y., et al., "CCTF Core I Test Results", presented at the Ninth Water Reactor Safety Research Information Meeting, Oct. (1981).
11. Rosal, E.R., et al., "FLECHT Low Flooding Rate Cosine Test Series Data Report", WCAP-8651 (1975).
12. Rosal, E.R., et al., "FLECHT Low Flooding Rate Skewed Test Series Data Report", WCAP-9018, May 1977.
13. Sudoh, T., et al., "Data Report on Series 4 Reflood Experiment", JAERI-M 7169, Aug. 1977 (in Japanese).
14. Sugimoto, J., et al., "Data Report on Series 5 Reflood Experiment", JAERI-M 7450, Jan. 1978 (in Japanese).
15. Iloeje, O.C., et al., "A Study of Wall Rewet and Heat Transfer in Dispersed Vertical Flow", MIT Report No.72718-92, 1974.
16. Marek, J. and Rehme, K., "Heat Transfer in Smooth Roughened Rod Bundles near Spacer Grids", Fluid Flow and Heat Transfer over Rod or Tuble Bundles, Edited S. Yao and P. Pfund, ASME 1978, p.163-170.

[Nomenclature]

D	:	Hydraulic diameter (m)
E	:	Emissivity (-)
H_{fg}	:	Latent heat of evaporation (kJ/kg)
h	:	Heat transfer coefficient ($W/m^2 K$)
L_q	:	Distance from the quench front (m)
Nu	:	Local Nusselt number with the spacer (-)
Nuo	:	Local Nusselt number without the spacer (-)
qw	:	Wall heat flux (W/m^2)
T	:	Temperature (K)
V	:	Velocity (m/sec)
x	:	Distance from the spacer (m)
α	:	Void fraction (-)
ΔT_{sat}	:	Wall superheat (K)
ε	:	Blockage ratio of the spacer (-)
λ	:	Thermal conductivity (W/m·K)
μ	:	Dynamic viscosity (kg/m·sec)
ρ	:	Density (kg/m^3)
σ	:	Stefan Blotzman constant ($W/m^2 K^4$)

Subscript

g	:	Gas phase
ℓ	:	Liquid phase
R	:	Radiation
sat	:	Saturated
w	:	Wall

Appendix A Plan of Grid Spacer Effect Experiment

A.1 Objectives

The objectives of the grid spacer effect experiment are as follows:

(1) to identify the heat transfer mechanism based on the flow observation near the grid spacers,

(2) to quantify the heat transfer enhancement caused by the grid spacers,

(3) to supply additional data for the different type of grid spacers, and

(4) to establish the method of analytical and experimental coupling between reflood facilities and PWRs concerning the effect of grid spacers.

A.2 Test Plan

To realize those objectives, a series of the experiment will be divided into four sections as shown in Fig.A.1. The circles in the figure show the locations of the view windows. The Core 0 has a basic configuration of the grid spacers (Type 1) and it will be utilized to get fundamental heat transfer data. The flow pattern just below the grid spacer will be observed at the midplane.

The Core 1 is a modification of the Core 0. The location of the central grid spacer will be shifted downward to observe the flow just above the grid spacer. The heat transfer data above the midplane will be compared with that of Core 1 as a function of the distance from the central grid spacer. Additional instrumentation will be supplied in the course of the modification to measure the wall temperature of the grid spacer at midplane and the vapor temperature in the core.

The Core 2 is the same as Core 1 except for the central grid spacer. The flow pattern and the heat transfer with no grid spacer at midplane will be compared with those of Core 1 to get the direct effect of the grid spacer. Also the additional heat transfer data as a function of the distance from the grid spacer will be obtained. Figure A.2 shows the location of the expected heat transfer data in the highest power region from Core 0 through Core 2.

In Core 3, all the grid spacers above midplane will be replaced

by the thinner grid spacers (Type 2) as were used in previous test series. The flow above midplane may be quite different due to the thinner grid spacers. The difference of the flow characteristics and the thermal hydraulic behavior in the upper part of the core will be analyzed for the analytical modeling of the grid spacer effect and for the coupling between the reflood test facilities and PWRs.

The specific features of the grid spacers used in Core 0 through Core 3 are summarized in Table A.1. Also the data of CCTF and FLECHT-SEASET[1] are listed for comparison. The blockage ratio of the grid spacer, ε, is defined as

$$\varepsilon = \frac{2\ell_p t - t^2}{\ell_p^2 - (\pi/4)d^2} \quad ,$$

where ℓ_p is the pitch of the heated rod, t is the thickness of the grid spacer, and d is the diameter of the heated rod.

A.3 Facility Description

(1) Layout

JAERI's small reflood test facility was designed to investigate the reflood phenomena during a LOCA of a PWR. The facility schematic is shown in Fig.A.3. The facility consists of a simulated core, lower and upper plenum, a downcomer, a primary loop, and additional supporting systems. The scaling factor based on the core flow area is about 1/1,000 of a 1,000 MWe class PWR.

(2) Test Section

Figure A.4 shows the cross section of the simulated core consisting of 32 electrically heated rods having a heated length of 3.6 m. Four non-heated rods are arranged at the corners. The core rod geometry is based on the 15 × 15 Westinghouse PWR design. The main specifications of the core design are listed in Table A.2. A water separator in the upper plenum removes the entrained water from the two-phase mixture from the core and drains the separated water into a tank to measure the entrainment rate.

(3) Downcomer

The downcomer pipe is connected to the test section lower plenum for the gravity feed reflood tests. The downcomer line will be bypassed for most of the test because the system effect is not the primary

objective of the present grid spacer experiment.

(4) Primary Loop

Two-phase mixture from the core exit is separated by the separator in the upper plenum, and the vapor mass flow discharges to the atmosphere via the primary loop. The primary loop consists of the simulated hot leg, the orifice plate to measure the mass flow rate, Containment 1, Containment 2, and the exhaust line. The flow area of the hot leg is 23.67 cm^2.

(5) Coolant Injection System

The coolant injection water is preheated in the 0.691 m^3 storage tank 1. The capacity of the main pump for the coolant injection is 3,600 m^3/hr maximum. The coolant is recirculating prior to the test through the storage tank, the lower plenum, the overflow nozzle at the lower plenum, and the storage tank. The constant or the stepped injection flow is accomplished by quick opening of the magnetic valve attached to the injection line.

A.4 Instrumentation

Instrumentation for the tests include heater rod thermocouples, fluid temperature thermocouples, structure wall thermocouples, absolute and differential pressure transducers, supplied power transducers and so on. The signals from the detectors are recorded on a digital magnetic tape for data reduction by the central computer.

(1) Heater Rod Thermocouples

The thermocouple to measure the clad surface temperature is burried in grooves on the outside surface of the heater rod. Figure A.5 shows the location of the instrumented rods and the elevation of the thermocouples. The thermocouples near the top of the heated length are intended to supply the information about the top quenching phenomena.

(2) Superheated Steam Probe

The location of the superheated steam probes is also shown in Fig.A.5. The superheated steam probes are all connected to the non-heated rods via guide plates as shown in Fig.A.6. The leading lines of the thermocouples are all burried on the surface of the non-heated rods. The thermocouple is an ungrounded type and the diameter is 0.5 mm. The information about the vapor superheat would be valuable for the model development of the grid spacer effects.

(3) Grid Spacer Wall Temperature

Two thermocouples are attached in the wall of the central grid spacer as shown in Fig.A.7. The leading lines of the thermocouples are burried on the surface of the non-heated rods. The grid spacer wall temperature will be utilized to evaluated the radiation heat transfer from the heater rod to the grid spacer and the timing of the rewetting of the grid spacer will be compared to the heat transfer augmentation near the grid spacer.

(4) Differential Pressures

Figure A.8 shows the schematic of the core differential pressure measurement in the core. The void fractions converted from the differential pressure measurement will be compared with the existing void fraction correlations for the reflood conditions[2]. The differential pressure with and without grid spacer between the pressure taps will be compared to estimate the frictional pressure loss at the spacers.

(5) Motion Picture

Motion pictures will be taken through the housing view windows to identify the flow patterns near the grid spacers for some selected runs. The time interval of the strobe light varies from ~1 μsec to ~10 μsec, and the frequency of the motion pictures is 24 frames per second coincident with the strobe light.

A.5 Test Procedure

Prior to the test, the rod bundle and its housing, and the coolant water are preheated to a specified temperature. In the forced flooding experiment, the coolant water is circulating through the line from the storage tank 1 to the lower plenum. After the establishment of the temperatures and the flow rate, the data recording system is turned on and the electric power is supplied to the heater rods. When the peak clad temperature reaches a pre-set value, the reflooding is initiated by quickly closing the valve in the overflow line, starting the water injection into the test section. After the whole core is quenched, the power is turned off and the data recording is stopped.

A.6 Test Conditions

Test conditions of the experiment is listed in Table A.3. The underline indicates the value of the base case. To avoid the failure of the heater rods or the thermocouples in the core, the thermally severe test case will be done at the last part of the test series. Although the detailed test matrix is not fixed, the tests will be run principly from the base case conditions with only one parameter varying at a time.

References in Appendix A

(1) Hochreiter, L.E., et al., "PWR FLECHT-SEASET Unblocked Bundle, Forced and Gravity Reflood Task: Task Plan Report", NRC/EPRI/ Westinghouse Report No.3, March, 1978.

(2) Iguchi, T., "Void Fraction in Simulated PWR Fuel Bundle during Reflood Phase", J. Nucl. Sci. Technol., 18 [12], 957～968 (1981).

Table A.1 Comparison of the structure of the grid spacer

Facility	Type	Thickness (mm)	Length (mm)	Blockage Ratio in Subchannel (%)
Core O-Core 2	Egg crate with dimples [Type 1]	0.8	40	19.4
Core 3 (upper part)	Egg crate with dimples [Type 2]	0.4	40	9.8
CCTF	Egg crate with strip holders	0.8	40	19.4
FLECHT-SEASET[15]	Egg crate with dimples	0.38	44.5	9.4

Table A.3 Test conditions of the experiments

System pressure (MPa)	0.1	0.2	0.4
Linear peak power (KW/m)	1.6	2.0	2.4
Flooding rate (cm/s)	1.5	2.0	4.0
Inlet water subcooling (°C)	20	50	80
Initial peak clad temperature (°C)	400	550	700
Housing wall superheat (°C)	0	100	200

Table A.2 Main specification of small scale reflood test facility

Bundle geometry	
Arrangement	6 × 6 -rod (Square pitch)
Number of heated rod	32
Number of non-heated rod	4
Outer diameter of rod	10.7×10^{-3}m
Pitch	14.3×10^{-3}m
Heated length	3.6 m
Core flow area	4.68×10^{-3} m^2
Heater rod design	
Type	Indirect heating type
Clad thickness	1.0×10^{-3}m
Clad material	Inconel - 600
Outer diameter of haeting element	6.4×10^{-3}m
Material of heating element	Nichrome
Attached thermocouple	0.5×10^{-3}m O.D. ungrounded type

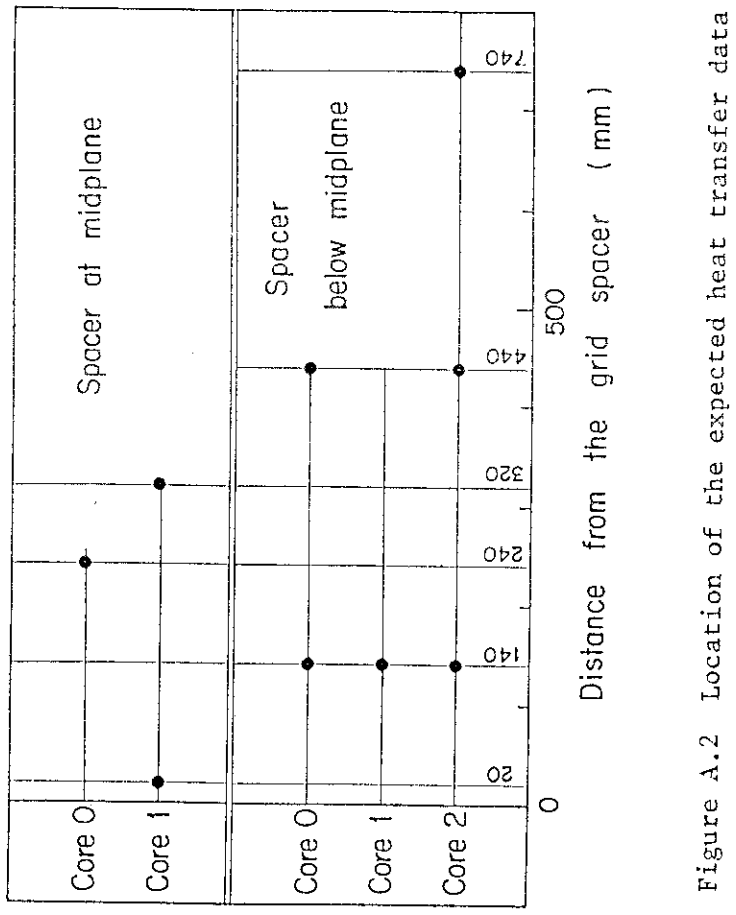

Figure A.2 Location of the expected heat transfer data

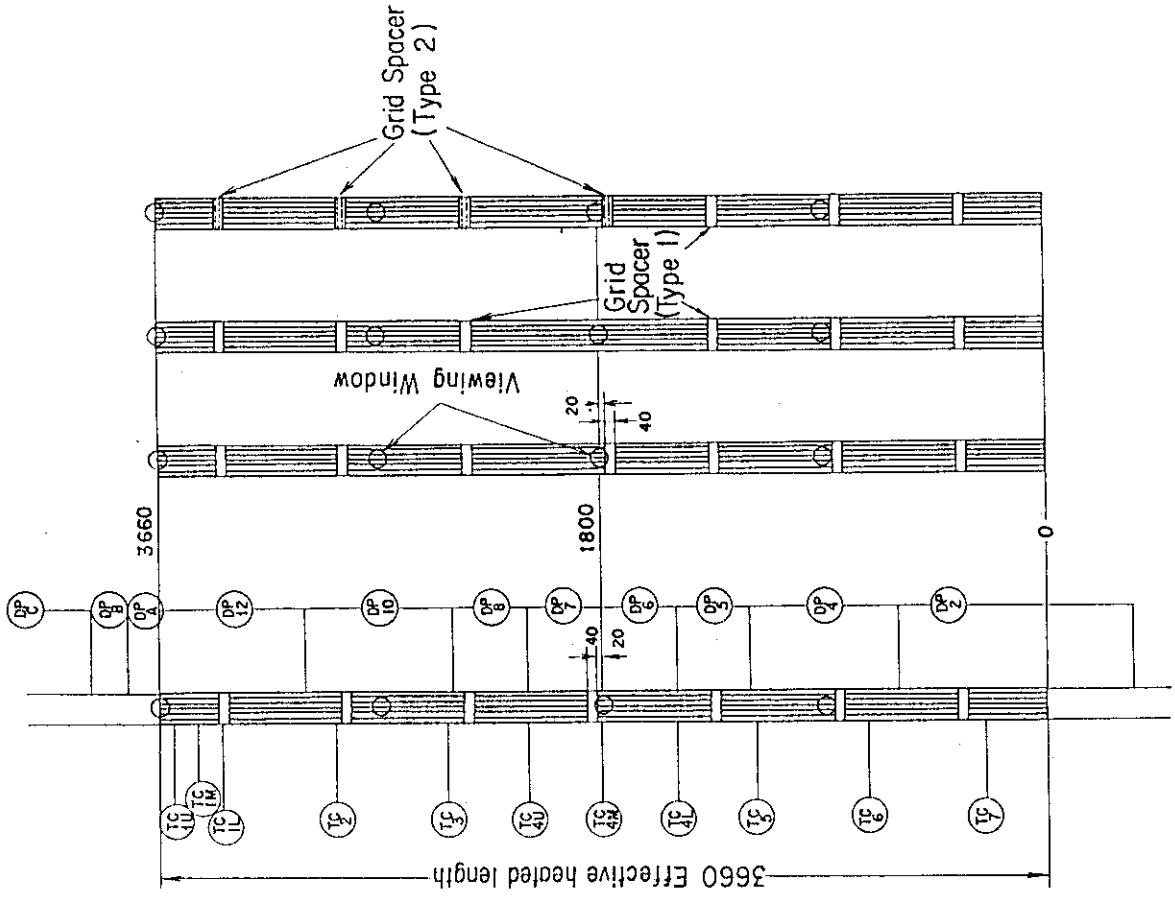

Figure A.1 Test plan and the main instrumentation

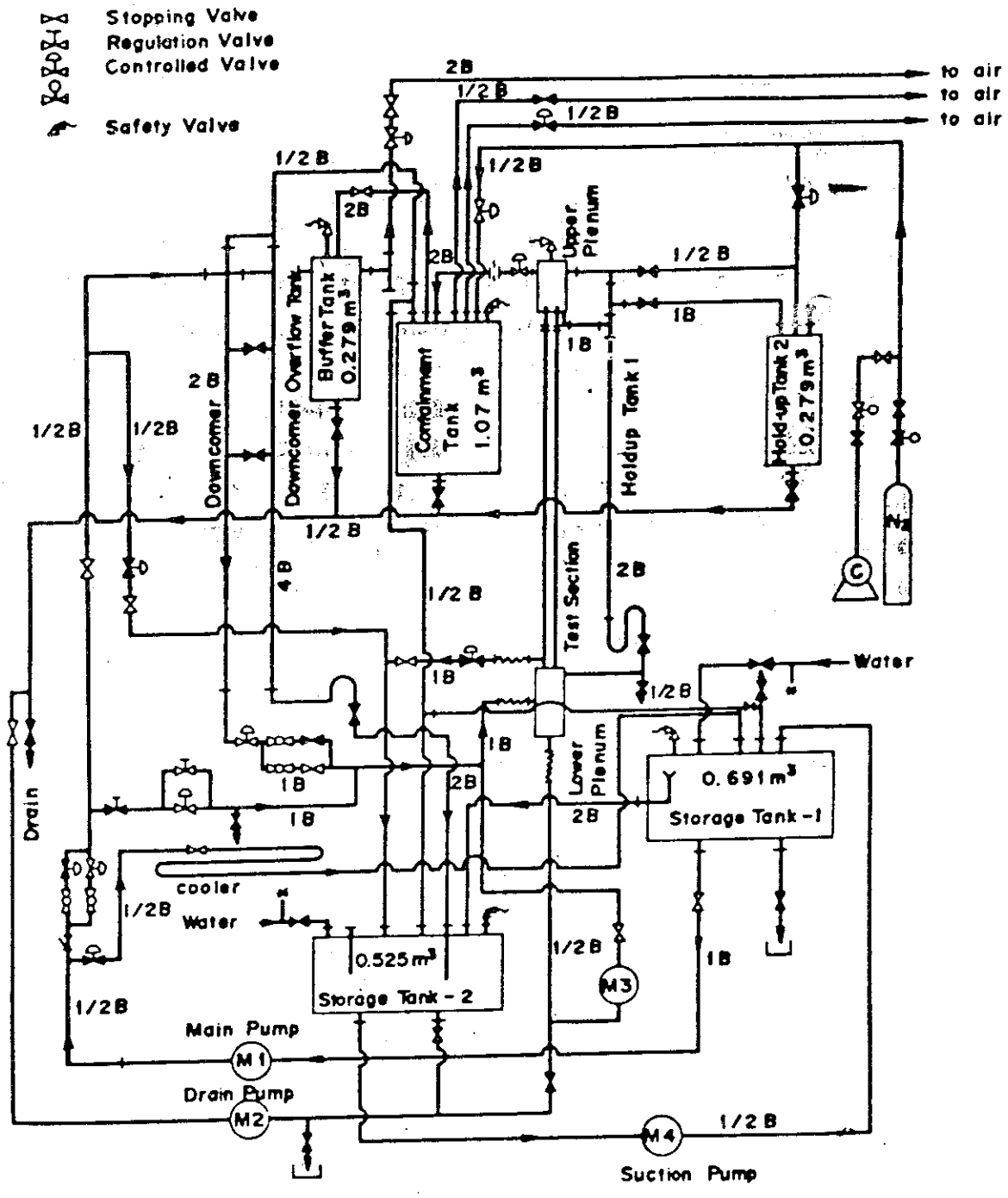

Figure A.3 Schematic of the test facility

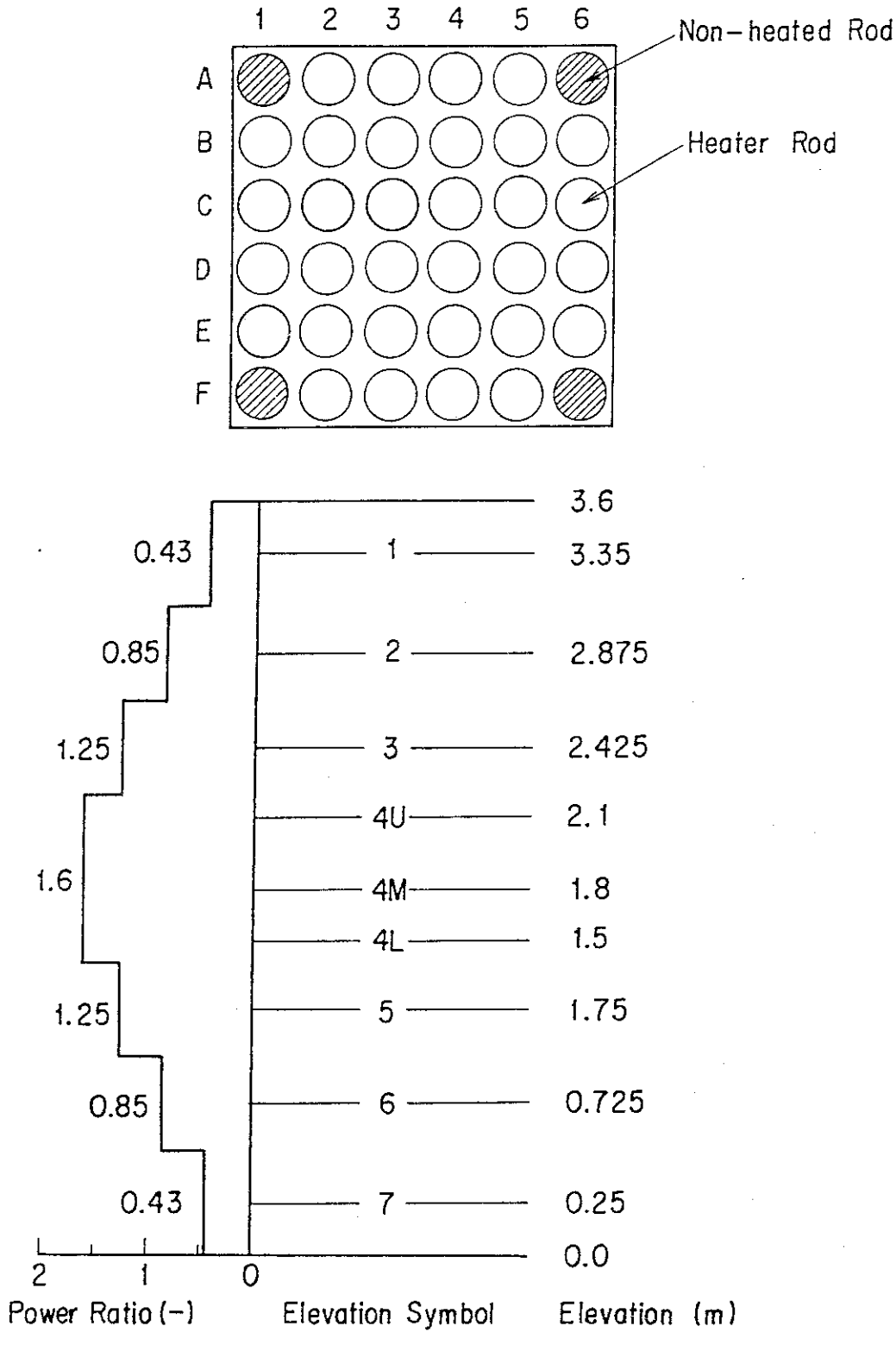

Figure A.4 Cross section and power distribution of the core

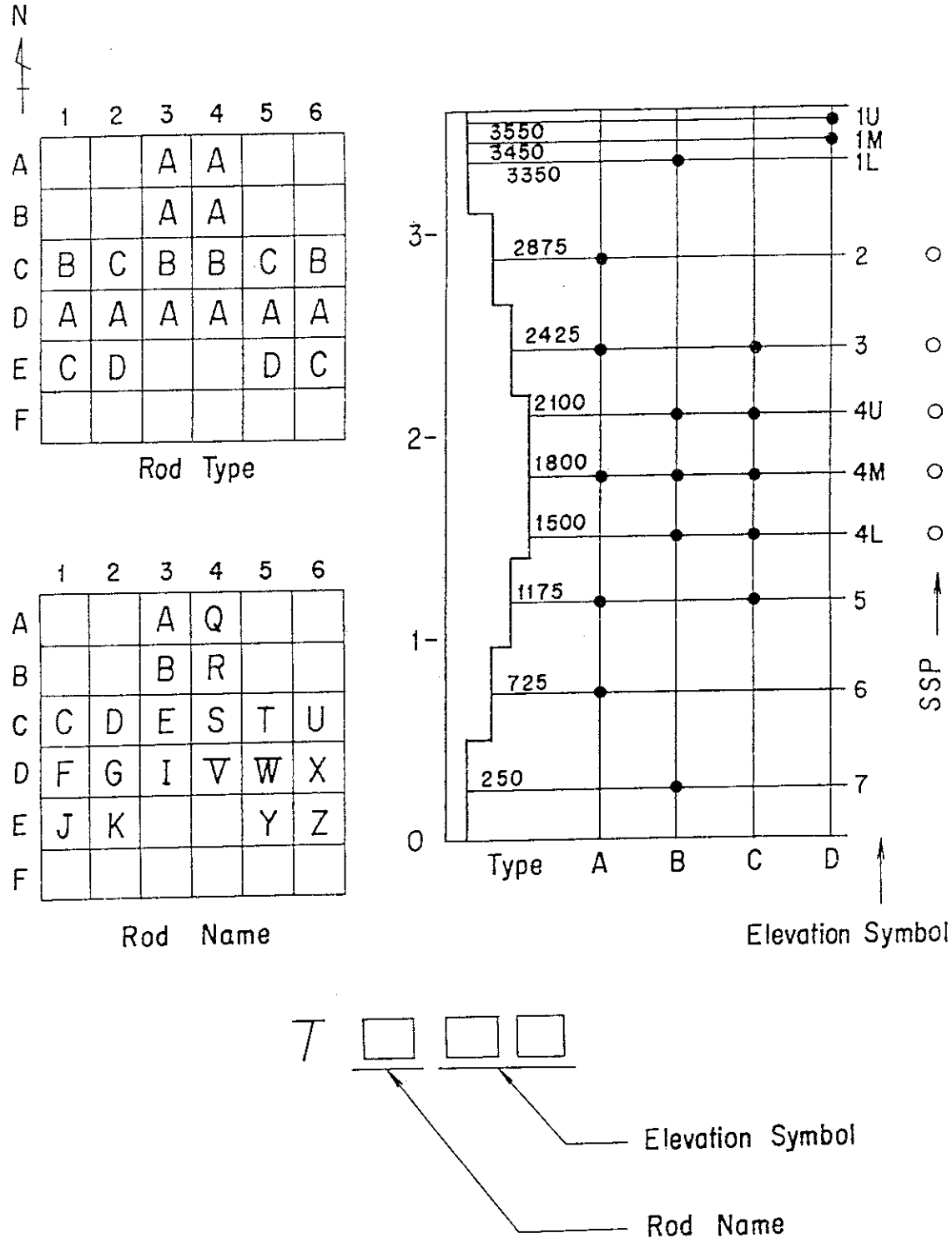

Figure A.5 Temperature measurement in the core

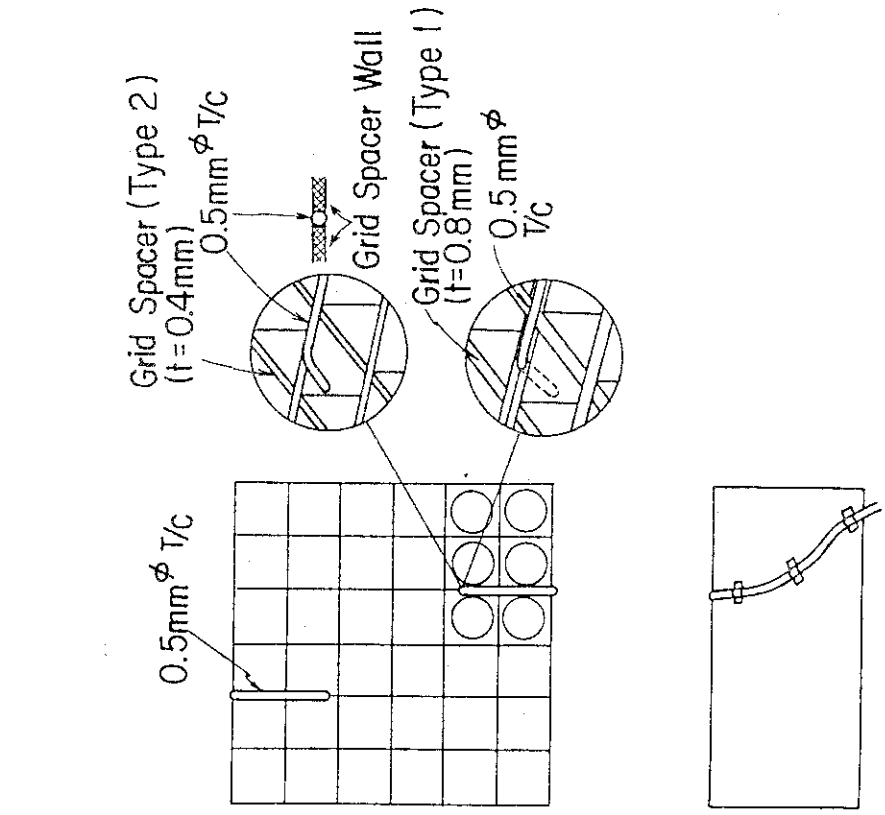

Figure A.7 Grid spacer thermocouple

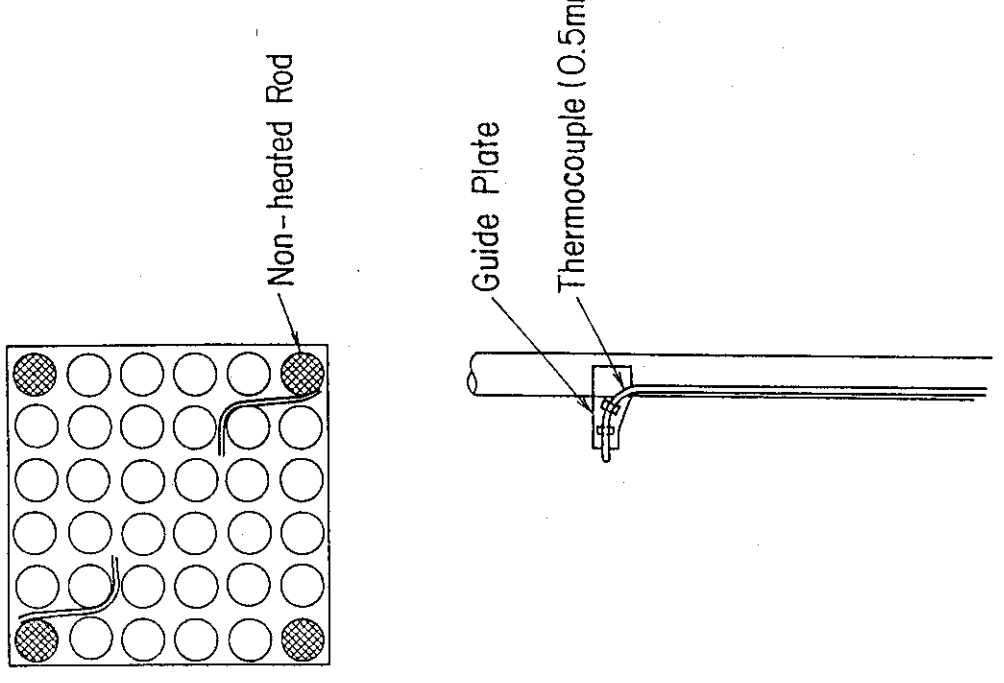

Figure A.6 Superheat steam probe

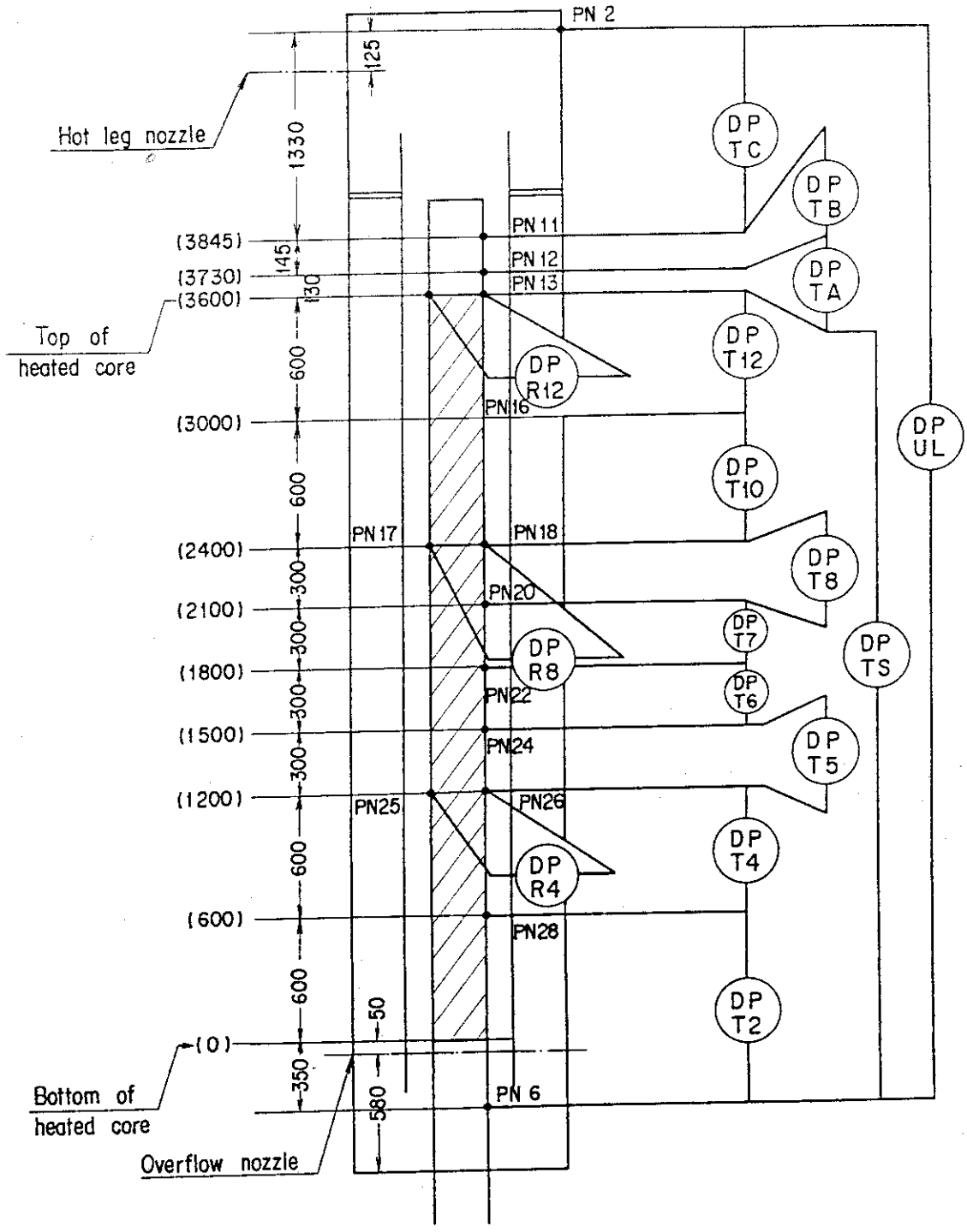

Figure A.8 Differential pressure measurement in the core